

000 001 002 003 004 005 006 007 008 009 010 011 012 013 014 015 016 017 018 019 020 021 022 023 024 025 026 027 028 029 030 031 032 033 034 035 036 037 038 039 040 041 042 043 044 045 046 047 048 049 050 051 052 053 FVBENCH: BENCHMARKING DEEPFAKE VIDEO DE- TECTION CAPABILITY OF LARGE MULTIMODAL MOD- ELS

006
007 **Anonymous authors**
008 Paper under double-blind review

011 ABSTRACT

013 As generative models rapidly evolve, the realism of AI-generated videos has
014 reached new levels, posing significant challenges for detecting the authenticity of
015 videos. Existing deepfake detection techniques generally rely on training datasets
016 with limited generation methods and content diversity, which limits their general-
017 ization ability on more realistic content, particularly that produced by the latest
018 generative models. Recently, large multimodal models (LMMs) have demon-
019 strated remarkable zero-shot performance across a variety of vision tasks. Yet,
020 their ability to discern deepfake videos remains largely untested. To this end, we
021 propose **FVBench**, a comprehensive deepfake **video benchmark** designed to ad-
022 vance video deepfake detection. It includes: **(i)** extensive content diversity, with
023 over 120K videos covering real, AI-edited, and fully AI-generated categories, **(ii)**
024 comprehensive model coverage, with fake videos generated and edited by 42 of
025 the state-of-the-art video synthesis and editing models, and **(iii)** deepfake video
026 detection benchmark for LMMs, which is a comprehensive benchmark for explor-
027 ing the deepfake video detection capabilities of LMMs. The FVBench dataset and
028 evaluation code will be publicly available upon publication, offering a valuable
029 resource for advancing deepfake detection.

030 1 INTRODUCTION

031
032 The rapid evolution of generative models has substantially increased the realism of AI-generated
033 videos, posing critical challenges for detecting digital content authenticity (Wang et al., 2025c;
034 Zhang et al., 2024d; Hou et al., 2024). Traditional deepfake detection techniques typically rely on
035 datasets with a limited number of generative models and relatively narrow content diversity (Chen
036 et al., 2024b; Bai et al., 2024). As a result, these models are often trained to detect artifacts specific
037 to a small set of manipulations. However, as the complexity and realism of AI-generated content
038 continue to grow (Wang et al., 2025b;d; Chen et al., 2024d), traditional models struggle to keep
039 up, leading to a decline in their ability to effectively detect modern deepfakes. Moreover, many of
040 the datasets used for training detection models are often outdated and no longer reflective of the
041 state-of-the-art generative capabilities (Khalid et al., 2021; Kuckreja et al., 2024; Yan et al., 2024),
042 making these models less reliable in real-world scenarios. Large Multimodal Models (LMMs) have
043 demonstrated impressive zero-shot capabilities across a wide range of vision tasks, such as face
044 recognition, object detection, and video captioning (Yang et al., 2025; Wang et al., 2025e; Xu et al.,
045 2025). These models have shown great potential to generalize across various tasks without the
046 need for task-specific fine-tuning (Bai et al., 2025; Li et al., 2024a;b). However, their potential for
047 deepfake detection remains largely unexplored.

048 Current deepfake video detection atsets and benchmarks for deepfake video detection suffer from
049 several critical shortcomings that limit their practical utility and generalization: (1) **Limited content**
050 **diversity**: most existing datasets concentrate primarily on facial forgeries, neglecting the growing
051 risk of non-facial manipulations (Kuckreja et al., 2024; Felouat et al., 2024; Yan et al., 2024). Fur-
052 thermore, many datasets are constructed under a binary real-or-fake paradigm (Hou et al., 2024;
053 Khalid et al., 2021; Zhang et al., 2024a), which lack partially AI-edited content where specific re-
gions are manipulated (Zhang et al., 2024c; Feng et al., 2024; Cohen et al., 2024). Additionally,
real videos often lack the natural distortions (e.g., compression artifacts, motion blur) commonly

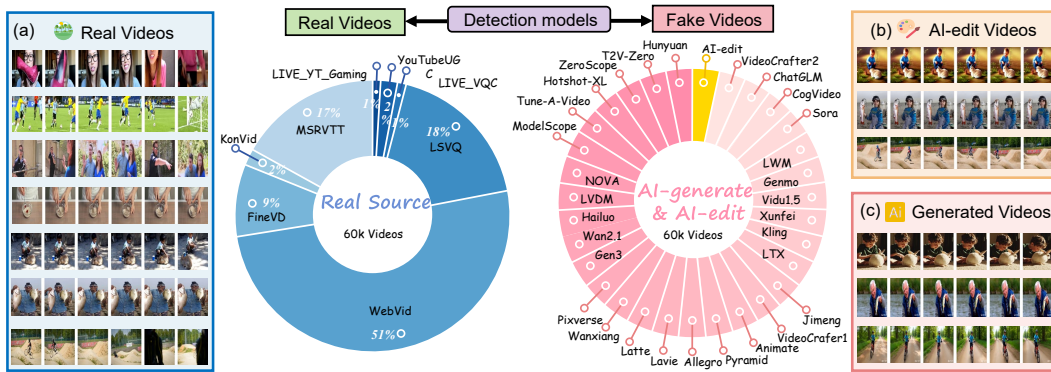


Figure 1: We present the FVBench, the large dataset for benchmarking deepfake video detection capabilities. (a) 60K real videos are collected from 8 sources. (b) 4K AI-edited videos using 12 editing models. (c) 60K fake videos are generated using 30 state-of-the-art generation models.

found in real-world scenarios (Hosu et al., 2017; Sinno & Bovik, 2018; Duan et al., 2025), which could improve robustness and generalization in detection models. (2) **Narrow model coverage**: existing datasets rely on a small number of generative models (Xie et al., 2022; Hou et al., 2024; Khalid et al., 2021), resulting in detection models learning model-specific artifacts rather than generalizable features indicative of manipulation. Additionally, older generative models often produce visible distortions, unnatural textures, or structural inconsistencies, making detection easier but hindering generalization to newer, more complex fakes generated by state-of-the-art models (Ma et al., 2025; Wang et al., 2025a; Team, 2024a;e). (3) **Restricted evaluation targets**: current benchmarks mainly assess specialized deepfake detection models, overlooking the emerging potential of LMMs in deepfake detection (Zhang et al., 2024d;a).

To this end, we introduce **FVBench**, a comprehensive deepfake video **benchmark** designed to overcome the limitations of existing datasets through three key contributions: (1) enhanced content diversity: FVBench includes not only fully synthetic, but also **partially manipulated videos** where only specific regions are edited. Furthermore, real videos incorporate natural distortions to enhance model robustness under realistic conditions. (2) expanded model coverage: fake videos include AI-generation videos using **30 models** and partial-AI videos edited by **12 AI-editing models**, covering a wide range of generation contents. (3) comprehensive evaluation framework: FVBench supports the evaluation of both the detection ability of conventional detectors and the LMMs. As illustrated in Figure 1, FVBench contains particularly deceptive examples that challenge deepfake detection models. In addition, Table 1 emphasizes the benchmark’s strengths in terms of dataset size, diversity, and the comprehensiveness of its evaluation framework when compared to existing resources.

In summary, our main contributions are:

- We introduce **FVBench**, the **largest** benchmark for deepfake video detection, including generation videos from 30 models, AI-edited videos from 12 models, and 8 real sources.
- We explore **LMMs** for deepfake video detection, conducting comprehensive benchmarks that assess their performance in detecting deepfakes across various video generation methods and content types.
- Through comprehensive experiments, we find the main challenge in current detection systems is the **zero-shot generalization ability** on previously unseen generation models. While detection models can achieve high performance on known generation models, the ability to generalize to unseen models remains a significant challenge.

2 RELATED WORK

A variety of datasets have been developed to advance deepfake video detection. Early efforts such as UADFV (Yang et al., 2019) and FaceForensics++ (Rossler et al., 2019) focused on facial forgeries. VFHQ (Xie et al., 2022), INDIFACE (Kuckreja et al., 2024), and FakeHumanVid (Zhang et al., 2024a) target “human-centric” forgeries, covering high-quality face swapping, specific ethnic faces,

108

109

Table 1: An overview of deepfake video detection datasets.

Dataset	Video Content	AI Generation Category		Public Availability	Database Real Sources	AI Models	Fake Videos	Total Videos
		Fully AI	Partial AI					
UADFV (Yang et al., 2019)	Face	✓	✗	✓	YouTube	1	252	493
FaceForensics++ (Rossler et al., 2019)	Face	✗	✓	✓	YouTube	4	4000	5000
VFHQ (Xie et al., 2022)	Face	✗	✓	✓	FFHQ Dataset	1	8000	16,000
INDIFACE (Kuckreja et al., 2024)	Face (Indian)	✓	✗	✓	YouTube	2	1,668	2,072
eKYC-DF (Felouat et al., 2024)	Face	✓	✗	✓	Private (Volunteers)	3	12,000	228,000
DF40 (Yan et al., 2024)	Face	✓	✗	✓	YouTube	Unknown	400,000	800,000
VIDEOSHAM (Mittal et al., 2022)	General	✗	✓	✓	Hollywood movies	-	413	826
PolyGlotFake (Hou et al., 2024)	Multimodal	✓	✗	✓	VoxCeleb 2	1	14,472	15,238
FakeAVCeleb (Khalid et al., 2021)	Multimodal	✓	✗	✓	VoxCeleb2	1	19,500	20,000
FakeHumanVid (Zhang et al., 2024a)	Human-centric	✓	✗	✓	TikTok, HDTF	9	7,600	15,000
IVY-FAKE (Zhang et al., 2024d)	General	✓	✓	✓	GenVideo, LOKI, YouTube	22	40,000	73,667
FVBench (Ours)	General	✓	✓	✓	8 Datasets	42	62,357	121,902

110

and full-body generation. FakeAVCeleb (Khalid et al., 2021) and PolyGlotFake (Hou et al., 2024) extend the challenge to multimodal domains by exploring audio-visual and multilingual forgeries, while IVY-FAKE (Zhang et al., 2024d) introduces a unified benchmark for explainable detection. Yet, critical gaps persist in existing benchmarks. Many datasets rely on a small or out-of-date set of generative models, making it difficult to generalize to more advanced model generation contents. Most benchmarks also focus on completely fake videos, ignoring the common issue of partially AI-edited content. Their collections of real videos are often pristine, lacking the natural distortions of real-world content and thus limiting the robustness of detection models. FVBench stands out for its scale, diversity, and balanced inclusion of real, AI-edited, and fully AI-generated videos from state-of-the-art models.

118

119

3 DATABASE CONSTRUCTION

120

121

3.1 REAL VIDEO COLLECTION

122

To ensure content diversity and realism, FVBench incorporates real videos from eight well-known public natural video datasets. These datasets are widely recognized for their diverse content and high-quality annotations, providing a solid foundation for deepfake detection across a broad range of scenarios. The MSRVTT (Xu et al., 2016) dataset includes 10,000 videos spanning various activities and is typically used for video-to-text tasks, while KonVid (Hosu et al., 2017) focuses on video quality assessment with 1,200 clips that capture various video distortions. FineVD (Duan et al., 2025) provides 5,074 videos with fine-grained annotations of distortions like noise and compression artifacts, ideal for training models on video quality degradation. The WebVid (Bain et al., 2021) dataset is scraped from the web, covering diverse content types like user-generated videos and news, making it perfect for video retrieval and action recognition tasks. LSVQ (Ying et al., 2021), with 10,759 video clips, offers real-world content for perceptual quality assessment, while LIVEVQC (Sinno & Bovik, 2018) focuses on videos impacted by network distortions in streaming scenarios. Additionally, YouTubeUGC (Wang et al., 2019) contributes 1,147 user-generated videos from the YouTube platform, covering a wide range of genres and providing rich content for scene detection and video quality tasks. Lastly, the LIVE-YT-Gaming (Yu et al., 2023) dataset, consisting of 600 gaming videos, caters to the gaming content genre. Collectively, these datasets ensure that FVBench includes a diverse mix of real-world videos, capturing a broad spectrum of quality, distortions, and content types to challenge deepfake detection models.

123

124

3.2 AI-EDITING VIDEO COLLECTION

125

126

We collect 180 base videos from Kinetics-400 (Kay et al., 2017) and DAVIS (Pont-Tuset et al., 2018) (50% human actions, 15% animal behaviors, 35% other). Editing prompts are generated using DeepSeek-R1 (DeepSeek-AI, 2025), covering five key tasks: color, action, background, object operation, and style change (e.g., oil painting, ink-style). These prompts were engineered to maintain 60% of the original content’s semantics, ensuring focused edits. We then use 12 open-source, diffusion-based video editing models including Tune-A-Video (Wu et al., 2023), TokenFlow (Qu et al., 2023), CCEdit (Feng et al., 2024), ControlVideo (Zhang et al., 2024c), FateZero (Qi et al., 2023), FLATTEN (Cong et al., 2024), FRESCO (Yang et al., 2024a), Pix2Video (Ceylan et al., 2023), RAVE (Kara et al., 2024), SlicEdit (Cohen et al., 2024), and Vid2Vid-Zero (Wang et al., 2024). Finally, we obtained 3,857 valid AI-edited videos.



Figure 2: Visualization of video frames in the FVBench dataset.

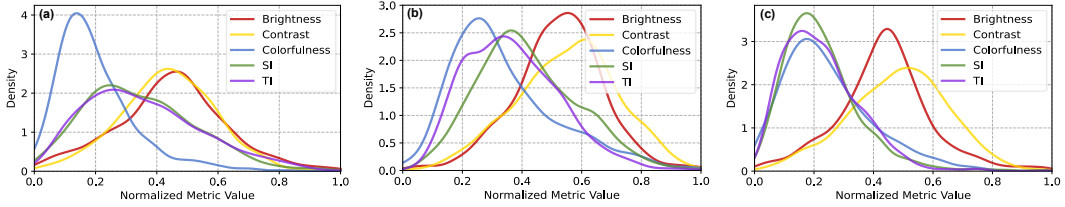


Figure 3: Feature distribution of the FVBench. (a) Feature distribution of real videos. (b) Feature distribution of AI-edited videos. (c) Feature distribution of AI-generated videos.

3.3 FAKE VIDEO GENERATION

To construct a diverse and challenging set of fake videos, we utilize 30 state-of-the-art video generation models, including 18 open-source generation models: Pyramid (Jin et al., 2024), Wan2.1 (Wang et al., 2025a), Allegro (Zhou et al., 2024), VideoCrafter2 (Chen et al., 2024a), CogVideo X1.5 (Yang et al., 2024b), Animate (Xu et al., 2024), Lavie (Wang et al., 2023b), Hotshot-XL (Mullan et al., 2023), Latte (Ma et al., 2025), VideoCrafter1 (Chen et al., 2023), Text2Video-Zero (Khachatryan et al., 2023), ModelScope (Wang et al., 2023a), Tune-A-Video (Wu et al., 2023), LTX (HaCohen et al., 2024), LVDM (He et al., 2022), ZeroScope (Team, 2024h), and LWM (Liu et al., 2024a) and 12 close-source generation models: Pixverse (AI, 2024), Wanxiang (Cloud, 2024), Hailuo (Team, 2024d), Jimeng (Team, 2024a), Hunyuan (Li et al., 2024c), Sora (Team, 2024e), Vidu1.5 (Team, 2024f), Gen3 (Runway, 2024), Kling (Team, 2024c), Genmo (Team, 2024b), ChatGLM (GLM et al., 2024), and Xunfei (Team, 2024g). To guarantee fairness, all generative models are used with their official default weights, with no additional adaptation or tuning.

The video prompts are mostly obtained from 8 existing open-domain text-video pair datasets, with some being refined using DeepSeek R1 (Guo et al., 2025) to ensure clarity and diversity. We use 2,750 distinct prompts in the training set; each prompt is processed by 18 open-source models. The test set includes 300 distinct prompts created by all 30 models. This approach generates 58,500 videos from 3,050 distinct prompts (2,750 prompts x 18 open-source models + 300 prompts x 30 models). The imbalance between the training and testing sets is due to two factors: (1) producing videos using close-source tools is expensive, and (2) we want to test the scalability of evaluation metrics on training-set unseen generation models. Figure 7 shows that all 30 models are given the same set of prompts based on real-world video captions. Some close-source models, such as Kling (Team, 2024c) and Hailuo (Team, 2024d), can provide highly detailed outputs that even surpass the real source.

3.4 DATABASE ANALYSIS

As shown in Figure 3, we analyze the feature distribution of real, AI-edited, and AI-generated videos in the FVBench dataset across five video quality-related features: colorfulness, brightness, contrast, spatial information (SI), and temporal information (TI). The analysis reveals that AI-generated videos display the highest values for SI and TI, indicating their rich spatial and temporal detail. In contrast, real videos exhibit greater colorfulness. AI-edited videos, which combine both authentic and manipulated content, show feature values that lie between the real and fake videos.

Table 2: **Performance benchmark on AI-generated video subsets.** \heartsuit Conventional deepfake detection models, \star open-source and \triangle close-source LMMs. \blacklozenge^* refers to finetuned models. We **bold** the best results.

Methods / Datasets	Gemmo	Hailuo	T2V-Zero	Tune-A-Video	LVDM	LWM	LTX	ZeroScope	Jimeng	VCrafter2	
\heartsuit Swin3D.T	74.00%	76.33%	67.67%	56.67%	66.00%	53.67%	61.00%	36.67%	68.67%	68.67%	
\heartsuit ResNet3D.18	82.00%	93.00%	95.00%	72.67%	73.00%	98.33%	78.67%	77.67%	92.33%	85.67%	
\heartsuit AIGVDet	83.74%	66.82%	91.49%	88.65%	62.78%	71.85%	59.32%	57.56%	48.56%	54.28%	
\heartsuit DeMamba	4.33%	0.33%	0.00%	2.00%	0.00%	10.67%	6.33%	2.67%	0.00%	0.33%	
\star Llava-one-vision (0.5B)	49.00%	41.00%	48.33%	47.67%	51.00%	48.67%	50.00%	48.00%	40.67%	49.00%	
\star InternVL2.5 (1B)	54.33%	50.33%	57.33%	58.00%	59.67%	59.00%	48.33%	49.00%	47.33%	51.67%	
\star InternVL3 (1B)	70.00%	56.00%	70.00%	65.67%	65.33%	67.33%	64.67%	63.33%	60.00%	62.33%	
\star Qwen2.5-VL (3B)	95.00%	98.33%	82.67%	87.00%	79.33%	80.67%	78.33%	79.00%	93.67%	87.00%	
\star VideoLlava (7B)	50.67%	49.00%	49.67%	50.00%	48.00%	46.33%	51.00%	50.33%	45.67%	49.00%	
\star Llava-one-vision (7B)	75.33%	38.00%	42.33%	60.33%	76.67%	63.67%	51.67%	48.00%	25.33%	36.33%	
\star mPLUG-Owl3 (7B)	86.67%	77.00%	74.00%	76.33%	94.33%	94.00%	83.33%	84.33%	51.00%	80.00%	
\star Qwen2.5-VL (7B)	89.33%	86.67%	82.00%	77.00%	64.67%	64.00%	62.33%	65.33%	77.67%	60.67%	
\star InternLM-XComposer2.5 (7B)	95.67%	95.67%	90.33%	94.00%	95.00%	89.67%	94.67%	97.67%	88.33%	94.67%	
\star VideoLlama3 (8B)	85.00%	78.33%	71.00%	48.33%	67.33%	61.67%	77.00%	68.33%	78.00%	59.00%	
\star Llava-NeXT-Video (8B)	53.33%	54.33%	53.67%	54.67%	66.00%	70.67%	62.67%	67.00%	43.00%	51.00%	
\star InternVL2.5 (8B)	88.00%	90.33%	75.00%	80.00%	69.67%	71.67%	72.00%	75.67%	79.33%	76.00%	
\star InternVL3 (9B)	89.00%	83.67%	77.00%	81.00%	78.33%	74.33%	80.00%	73.67%	81.67%	76.00%	
\star Llama3.2-Vision (11B)	84.00%	79.00%	79.00%	71.67%	76.33%	66.33%	77.33%	73.67%	74.33%	82.33%	
\star InternVL2.5 (26B)	60.67%	72.67%	61.33%	63.67%	69.33%	64.33%	63.33%	64.00%	60.00%	60.33%	
\star Qwen2.5-VL (32B)	76.67%	80.33%	71.67%	69.00%	45.33%	56.00%	54.00%	65.67%	70.67%	65.33%	
\star InternVL2.5 (38B)	70.67%	67.33%	67.67%	69.67%	62.00%	69.67%	64.67%	60.33%	62.00%	62.00%	
\star InternVL3 (38B)	81.00%	84.33%	80.67%	79.33%	74.00%	74.33%	70.67%	67.67%	81.67%	64.33%	
\star Qwen2.5-VL (72B)	93.00%	93.00%	80.33%	71.33%	51.33%	54.33%	51.33%	52.33%	79.33%	57.00%	
\star InternVL3 (78B)	69.00%	80.00%	72.00%	76.00%	66.67%	72.67%	63.67%	54.67%	68.00%	57.33%	
\triangle Gemini.1.5-pro	98.33%	81.67%	98.33%	95.00%	81.67%	75.00%	66.67%	95.00%	91.67%	-	
\triangle GPT4o	100.0%	65.00%	86.67%	88.33%	71.67%	76.67%	68.33%	46.67%	46.67%	93.33%	
Model Average (Zero-shot)	73.35%	70.49%	68.34%	66.69%	65.09%	65.99%	63.53%	61.95%	63.15%	62.09%	
\diamond Swin3D.T*	100.0%	100.0%	100.0%	100.0%	100.0%	100.0%	100.0%	100.0%	100.0%	100.0%	
\diamond ResNet3D.18*	100.0%	100.0%	100.0%	100.0%	100.0%	100.0%	100.0%	100.0%	100.0%	100.0%	
\blacklozenge InternVL2.5 (8B)*	100.0%	100.0%	100.0%	100.0%	100.0%	100.0%	100.0%	100.0%	100.0%	100.0%	
\blacklozenge InternVL3 (9B)*	100.0%	100.0%	100.0%	100.0%	100.0%	100.0%	100.0%	100.0%	100.0%	100.0%	
Methods / Datasets	Xunfei	Hotshot	Junyuan	CogVideo	NOVA	VCrafter1	Sora	ChatGLM	Wan2.1	Animate	
\heartsuit Swin3D.T	83.67%	52.33%	73.00%	60.00%	63.67%	58.00%	64.67%	61.00%	61.33%	66.33%	
\heartsuit ResNet3D.18	86.00%	71.00%	74.00%	84.67%	78.67%	97.33%	85.33%	89.67%	89.67%	86.67%	
\heartsuit AIGVDet	49.45%	53.24%	71.51%	21.57%	72.48%	21.30%	76.45%	46.67%	74.35%	23.81%	
\heartsuit DeMamba	0.67%	8.33%	0.33%	13.67%	13.67%	0.00%	0.67%	0.00%	1.00%	16.67%	
\star Llava-one-vision (0.5B)	48.33%	48.00%	42.33%	47.33%	47.67%	48.33%	45.67%	46.33%	45.67%	46.67%	
\star InternVL2.5 (1B)	52.67%	49.33%	42.33%	51.67%	45.33%	56.33%	49.33%	48.00%	48.00%	48.67%	
\star InternVL3 (1B)	58.33%	62.67%	51.67%	58.00%	55.67%	57.00%	59.00%	59.67%	57.33%	56.67%	
\star Qwen2.5-VL (3B)	83.33%	71.00%	82.67%	72.67%	68.33%	64.00%	70.33%	66.67%	75.67%	47.33%	
\star VideoLlava (7B)	45.67%	47.33%	46.00%	50.00%	48.67%	48.00%	48.67%	48.33%	46.33%	48.33%	
\star Llava-one-vision (7B)	23.33%	32.00%	16.00%	30.67%	36.33%	35.67%	20.00%	30.33%	19.67%	23.00%	
\star mPLUG-Owl3 (7B)	59.33%	68.67%	51.67%	62.67%	71.67%	72.33%	45.67%	52.67%	42.33%	54.33%	
\star Qwen2.5-VL (7B)	52.33%	41.00%	48.67%	45.67%	38.33%	40.33%	50.00%	42.00%	43.67%	32.33%	
\star InternLM-XComposer2.5 (7B)	90.33%	99.00%	84.00%	95.33%	96.33%	95.67%	93.67%	90.67%	92.00%	93.00%	
\star VideoLlama3 (8B)	64.33%	60.67%	78.00%	67.00%	63.67%	55.33%	68.00%	65.67%	63.33%	58.33%	
\star Llava-NeXT-Video (8B)	46.67%	51.67%	44.67%	51.67%	51.33%	56.33%	47.67%	46.33%	43.00%	44.33%	
\star InternVL2.5 (8B)	67.67%	63.67%	78.33%	63.33%	63.67%	53.33%	61.33%	62.33%	61.33%	62.33%	
\star InternVL3 (9B)	68.33%	69.00%	70.00%	71.67%	70.00%	67.00%	64.67%	66.67%	68.67%	58.00%	
\star Llama3.2-Vision (11B)	81.00%	77.00%	72.67%	74.67%	73.33%	79.33%	77.67%	83.67%	79.67%	67.33%	
\star InternVL2.5 (26B)	50.33%	56.67%	59.33%	56.33%	58.67%	63.00%	47.33%	49.33%	48.33%	57.00%	
\star Qwen2.5-VL (32B)	64.33%	46.33%	48.67%	39.67%	37.00%	47.33%	52.33%	39.00%	44.67%	31.67%	
\star InternVL2.5 (38B)	48.00%	51.33%	53.00%	53.00%	50.00%	41.33%	39.67%	47.00%	47.67%	44.00%	
\star InternVL3 (38B)	66.67%	64.33%	64.67%	63.67%	65.33%	53.67%	59.33%	62.00%	64.67%	52.00%	
\star Qwen2.5-VL (72B)	41.00%	41.67%	50.33%	34.00%	33.67%	35.00%	59.33%	35.67%	43.67%	27.00%	
\star InternVL3 (78B)	47.00%	49.00%	55.00%	50.67%	44.67%	49.33%	42.00%	49.00%	44.00%	41.00%	
\triangle Gemini.1.5-pro	58.33%	68.33%	83.33%	43.33%	66.67%	73.33%	85.00%	35.00%	46.67%	25.00%	
\triangle GPT4o	45.00%	30.00%	26.67%	30.00%	46.67%	36.67%	16.67%	26.67%	35.00%	15.00%	
Model Average (Zero-shot)	57.45%	55.64%	56.62%	54.98%	56.17%	53.97%	53.57%	50.39%	54.42%	49.45%	
\diamond Swin3D.T*	100.0%	100.0%	100.0%	100.0%	100.0%	100.0%	100.0%	100.0%	100.0%	100.0%	
\diamond ResNet3D.18*	100.0%	100.0%	100.0%	100.0%	100.0%	100.0%	100.0%	100.0%	100.0%	100.0%	
\blacklozenge InternVL2.5 (8B)*	100.0%	100.0%	100.0%	100.0%	100.0%	100.0%	100.0%	100.0%	100.0%	100.0%	
\blacklozenge InternVL3 (9B)*	100.0%	100.0%	100.0%	100.0%	100.0%	100.0%	100.0%	100.0%	100.0%	100.0%	
Methods / Datasets	Wanxiang	Allegro	Pyramid	Vidu1.5	Lavie	Kling	Pixverse	Latte	MScope	Gen3	Overall
\heartsuit Swin3D.T	75.33%	73.00%	78.33%	75.33%	58.33%	66.33%	68.67%	58.33%	53.67%	70.52%	65.04%
\heartsuit ResNet3D.18	80.67%	85.33%	83.00%	79.33%	82.00%	81.33%	85.00%	79.67%	72.00%	85.01%	80.85%
\heartsuit AIGVDet	39.23%	91.07%	0.00%	42.45%	48.97%	46.32%	53.45%	68.95%	59.56%	67.59%	57.12%
\heartsuit DeMamba	0.33%	3.00%	2.33%	0.67%	3.00%	1.33%	0.33%	6.00%	0.00%	0.40%	3.30%
\star Llava-one-vision (0.5B)	48.00%	48.00%	47.33%	49.00%	46.00%	47.33%	47.00%	48.00%	50.33%	47.41%	47.27%
\star InternVL2.5 (1B)	44.67%	41.67%	46.67%	47.33%	53.67%	43.33%	49.00%	52.33%	57.00%	50.00%	50.41%
\star InternVL3 (1B)	57.67%	63.00%	58.00%	59.00%	67.00%	53.00%	55.67%	59.00%	67.33%	59.36%	60.66%
\star Qwen2.5-VL (3B)	97.33%	87.67%	85.00%	87.00%	72.00%	92.00%	76.67%	71.33%	86.65%	79.67%	-
\star VideoLlava (7B)	47.67%	50.33%	46.00%	52.67%	49.00%	42.00%	47.67%	48.33%	49.80%	48.23%	-
\star Llava-one-vision (7B)	23.00%	33.33%	32.00%	36.67%	38.67%	22.00%	27.33%	36.67%	20.12%	35.88%	-
\star mPLUG-Owl3 (7B)	66.00%	75.33%	61.00%	77.67%	61.00%	61.67%	66.67%	64.33%	75.67%	49.20%	68.03%
\star Qwen2.5-VL (7B)	55.33%	64.00%	67.00%	62.00%	53.33%	52.67%	51.67%	49.67%	38.67%	54.58%	57.10%
\star InternLM-XComposer2.5 (7B)	89.67%	93.00%	93.67%	93.33%	93.00%	90.00%	91.67%	91.00%	94.00%	94.42%	92.98%
\star VideoLlama3 (8B)	75.00%	69.67%	66.67%	70.67%	65.00%	75.33%	65.00%	66.33%	58.00%	60.16%	67.01%
\star Llava-NeXT-Video (8B)	47.00%	53.33%	46.67%	49.00%	53.00%	44.67%	46.33%	49.00%	59.67%	49.80%	51.95%
\star InternVL2.5 (8B)	85.67%	73.33%	65.33%	76.33%	68.00%	81.33%	70.00%	67.00%	61.67%	65.34%	70.97%
\star InternVL3 (9B)	81.00%	70.00%	73.00%	79.67%	72.00%	78.33%	74.00%	74.00%	70.72%	73.79%	-
\star Llama3.2-Vision (11B)	77.00%	78.33%	77.33%	79.33%	78.33%	78.67%	82.33%	79.00%	77.67%	74.30%	77.09%
\star InternVL2.5 (26B)	57.33%	56.00%	59.33%	59.00%	59.33%	57.00%	50.33%	57.67%	54.00%	52.39%	58.28%
\star Qwen2.5-VL (32B)	59.00%	58.33%	68.67%	50.00%	57.33%	41.00%	64.67%	48.67%	44.67%	59.36%	55.25%
\star InternVL2.5 (38B)	64.00%	54.00%	51.33%	54.67%	54.00%	52.00%	52.33%	54.33%	58.00%	44.82%	55.72%
\star InternVL3 (38B)	70.67%	73.33%	75.33%	62.00%	62.33%	65.33%	64.00%	62.33%	64.00%	65.74%	67.98%
\star Qwen2.5-VL (72B)	62.33%										

270

271
272
273
Table 3: **Performance benchmark on real video subsets.** \heartsuit Conventional deepfake detection mod-
els, \star open-source and \triangle close-source LMMs. \blacklozenge^* refers to finetuned models. We **bold** the best
results.

Methods / Datasets	MSRVTT	KoNViD	FineVD	WebViD	LSVQ	LIVEVQC	YouTubeUGC	LIVE-YT-Gaming	Overall
\heartsuit Swin3D-T	58.95%	54.58%	67.83%	70.97%	55.86%	63.25%	73.25%	80.00%	65.47%
\heartsuit ResNet3D_18	84.45%	85.83%	86.78%	94.12%	82.85%	90.60%	89.04%	82.50%	89.56%
\heartsuit AIGVDet	100.0%	98.75%	93.97%	89.86%	93.12%	93.16%	84.84%	89.17%	92.74%
\heartsuit DeMamba	99.90%	98.75%	99.41%	99.95%	84.34%	100.0%	100.0%	98.33%	97.03%
\star Llava-one-vision (0.5B)	59.35%	62.50%	55.91%	50.25%	58.32%	60.68%	57.89%	50.00%	56.86%
\star InternVL2.5 (1B)	68.80%	59.17%	49.90%	67.60%	58.27%	54.70%	59.21%	54.17%	58.98%
\star Qwen2.5-VL (3B)	53.00%	79.58%	27.85%	58.66%	72.15%	82.91%	52.19%	45.00%	58.92%
\star VideoLlava (7B)	59.30%	57.92%	48.72%	56.67%	60.69%	54.82%	54.45%	35.00%	53.45%
\star Llava-one-vision (7B)	80.25%	96.25%	62.40%	86.67%	91.03%	100.00%	69.74%	45.00%	78.92%
\star mlPLUG-Owl3 (7B)	47.35%	78.33%	19.98%	78.32%	78.39%	91.45%	48.68%	2.50%	55.63%
\star Qwen2.5-VL (7B)	70.80%	93.75%	49.21%	62.78%	88.29%	63.16%	83.43%	15.83%	65.91%
\star InternLM-XComposers2.5 (7B)	65.75%	76.67%	51.87%	62.73%	72.58%	65.81%	45.61%	55.83%	62.11%
\star VideoLlama3 (8B)	50.45%	59.17%	29.63%	41.67%	57.48%	39.04%	50.23%	30.00%	44.71%
\star LLaVA-NeXT-Video (8B)	53.65%	65.00%	44.00%	42.67%	59.34%	61.54%	50.00%	39.17%	51.92%
\star InternVL2.5 (8B)	52.55%	71.67%	38.48%	57.93%	67.01%	78.63%	49.56%	34.17%	56.25%
\star InternVL3 (9B)	44.20%	63.75%	29.63%	51.31%	56.51%	69.23%	41.67%	22.50%	47.35%
\star Llama3.2-Vision (11B)	24.05%	38.33%	20.47%	25.79%	33.04%	50.43%	25.44%	14.17%	28.97%
\star InternVL2.5 (26B)	65.40%	62.92%	46.75%	51.15%	67.47%	73.50%	60.96%	38.33%	58.31%
\star Qwen2.5-VL (32B)	70.05%	96.25%	56.89%	85.02%	89.50%	99.15%	72.90%	30.83%	75.07%
\star InternVL2.5 (38B)	68.50%	80.42%	47.15%	74.06%	80.81%	90.60%	61.84%	24.17%	65.94%
\star InternVL3 (38B)	68.60%	84.58%	39.96%	77.98%	79.04%	91.45%	60.53%	12.50%	64.33%
\star Qwen2.5-VL (72B)	83.10%	97.08%	68.90%	86.62%	92.57%	100.00%	77.34%	39.17%	80.60%
\star InternVL3 (78B)	75.70%	93.33%	57.09%	75.71%	87.50%	97.44%	72.81%	33.33%	74.11%
\triangle Gemini1.5-pro	90.00%	100.0%	80.00%	76.67%	93.10%	100.0%	69.57%	50.88%	79.91%
\triangle GPT-4o	90.00%	96.67%	75.00%	88.14%	93.22%	100.0%	78.26%	63.33%	72.10%
Model Average (Zero-shot)	64.66%	75.00%	51.62%	66.72%	71.36%	75.95%	61.86%	42.67%	63.84%
\blacklozenge Swin3D-T*	94.25%	65.62%	82.27%	96.93%	75.42%	67.74%	86.96%	92.71%	86.03%
\blacklozenge ResNet3D_18*	99.88%	100.0%	98.65%	100.0%	98.78%	100.0%	100.0%	100.0%	99.41%
\blacklozenge InternVL2.5 (8B)*	100.0%	98.44%	99.38%	100.0%	99.30%	100.0%	97.83%	100.0%	99.62%
\blacklozenge InternVL3 (9B)*	99.69%	97.40%	97.41%	86.63%	98.19%	99.98%	86.96%	100.0%	95.23%

292
293
4 BENCHMARK AND EVALUATION294
295
We benchmark and evaluate both the in-domain performance and cross-generator generalization of
various deepfake detection models across three subsets: real, AI-edited, and AI-generated videos.296
297
4.1 EXPERIMENT SETUP298
299
300
We evaluate the models' ability to classify real and fake videos using two standard metrics: accuracy
(Acc) and F1-score. Accuracy is calculated as the proportion of correctly classified real or fake
videos out of all relevant samples in the dataset.301
302
To provide a more balanced evaluation that accounts for both precision and recall, we also compute
the F1-score, which is the harmonic mean of precision and recall:

303
304
305
$$F1 = \frac{2 \times \text{Precision} \times \text{Recall}}{\text{Precision} + \text{Recall}} \quad (1)$$

306
where precision and recall are:

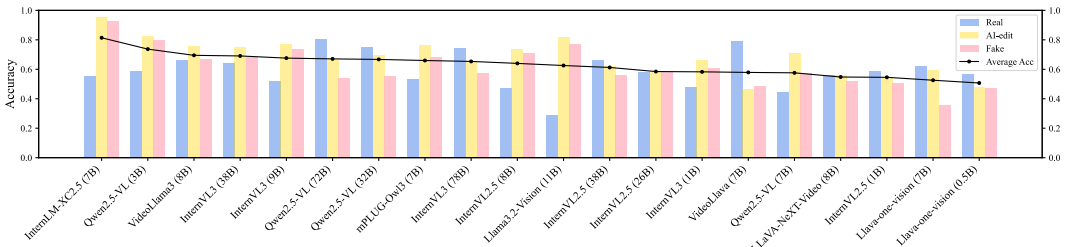
307
308
$$\text{Precision} = \frac{\text{TP}}{\text{TP} + \text{FP}}, \quad \text{Recall} = \frac{\text{TP}}{\text{TP} + \text{FN}} \quad (2)$$

309
310
311
312
313
314
315
316
317
318
319
320
321
322
323
where TP (True Positives) represents the number of real or fake videos correctly identified by the
model, and FN (False Negatives) indicates the number of videos incorrectly classified as the op-
posite category. We directly use publicly available pre-trained weights to conduct inference on the
test datasets. For large multimodal models (LMMs), we perform inference using a prompt-based
question-answering approach. To minimize any bias in the responses, we alternate between the fol-
lowing two instructions: (1) "Is this a real video or a generated video? Just answer with A or B. A:
real or B: generated." and (2) "Is this a generated video or a real video? Just answer with A or B.
A: generated or B: real." Additionally, we fine-tune two of the LMMs with LoRA (Hu et al., 2022)
(r=16), using the same 4:1 training and testing split. The fine-tuning process is conducted over 5
epochs. The models are implemented in PyTorch and trained on a 40GB NVIDIA RTX A6000 GPU
with a batch size of 4. The initial learning rate is set to 1e-5 and is adjusted using a cosine annealing
strategy.321
322
4.2 IN-DOMAIN PERFORMANCE ON FVBENCH323
We benchmark model performance on AI-generated video subsets, as shown in Table 2. We can ob-
serve that traditional deep learning-based detection models, such as DeMamba (Chen et al., 2024b)

324

325 **Table 4: Performance benchmark on AI-edit video subsets, including five editing types.** ♦*
326 refers to finetuned models.

Dimension Methods / Metrics	Background Acc(%) \uparrow	F1 \uparrow	Style Change Acc(%) \uparrow	F1 \uparrow	Color Change Acc(%) \uparrow	F1 \uparrow	Action Edit Acc(%) \uparrow	F1 \uparrow	Object Operation Acc(%) \uparrow	F1 \uparrow	Overall Acc(%) \uparrow	F1 \uparrow
♡Swin3D-T	59.42	0.745	53.03	0.693	52.10	0.685	61.76	0.764	45.76	0.628	53.18	0.694
♡ResNet3D-18	86.78	0.929	85.71	0.923	87.80	0.935	85.12	0.92	86.46	0.927	86.53	0.928
♡AIGVDet	82.95	0.820	84.39	0.827	73.36	0.771	82.02	0.816	76.44	0.787	79.83	0.804
♡DeMamba	0.000	0.000	0.000	0.000	0.000	0.000	0.000	0.000	0.000	0.000	0.000	0.000
★Llava-one-vision (0.5B))	51.24	0.678	48.12	0.650	49.76	0.664	42.98	0.601	46.88	0.638	47.93	0.611
★InternVL2.5 (1B)	58.68	0.740	58.65	0.739	52.20	0.686	52.07	0.685	52.08	0.685	54.27	0.659
★InternVL3 (1B)	57.02	0.726	68.42	0.813	67.80	0.808	60.33	0.753	71.88	0.836	66.06	0.740
★Qwen2.5-VL (3B)	84.30	0.915	85.71	0.923	87.80	0.935	68.60	0.814	82.29	0.903	82.51	0.847
★VideoLlava (7B)	48.76	0.656	42.86	0.600	52.68	0.690	38.02	0.551	46.35	0.633	46.50	0.594
★Llava-one-vision (7B)	57.85	0.733	76.69	0.868	61.46	0.761	38.02	0.551	60.94	0.757	59.72	0.727
★mPLUG-Owl3 (7B)	73.55	0.848	81.95	0.901	83.90	0.912	58.68	0.740	77.60	0.874	76.42	0.829
★Qwen2.5-VL (7B)	71.07	0.831	76.69	0.868	81.95	0.901	42.98	0.601	72.92	0.843	70.98	0.790
★InternLM-XComposer2.5 (7B)	94.21	0.970	96.24	0.981	94.15	0.970	96.69	0.983	96.88	0.984	95.60	0.958
★VideoLlama3 (8B)	70.25	0.825	82.71	0.905	82.44	0.904	59.50	0.746	76.56	0.867	75.52	0.799
★LLaVA-NeXT-Video (8B)	57.02	0.726	55.64	0.715	60.49	0.754	48.76	0.656	55.73	0.716	56.09	0.677
★InternVL2.5 (8B)	65.29	0.790	81.95	0.901	82.93	0.907	57.02	0.726	73.96	0.850	73.70	0.789
★InternVL3 (9B)	77.69	0.874	84.96	0.919	80.98	0.895	61.16	0.759	77.08	0.871	77.07	0.812
★Llama3.2-Vision (11B)	80.17	0.890	86.47	0.927	84.88	0.918	77.69	0.874	78.12	0.877	81.61	0.826
★InternVL2.5 (26B)	52.89	0.692	65.41	0.791	60.49	0.754	55.37	0.713	58.33	0.737	58.81	0.700
★Qwen2.5-VL (32B)	61.16	0.759	73.68	0.848	82.93	0.907	44.63	0.617	74.48	0.854	69.82	0.780
★InternVL2.5 (38B)	55.37	0.713	68.42	0.813	70.73	0.829	43.80	0.609	64.06	0.781	62.05	0.732
★InternVL3 (38B)	73.55	0.848	78.20	0.878	80.98	0.895	54.55	0.706	79.69	0.887	74.87	0.815
★Qwen2.5-VL (72B)	61.16	0.759	75.94	0.863	76.10	0.864	41.32	0.585	68.75	0.815	66.45	0.760
★InternVL3 (78B)	58.68	0.740	74.44	0.853	72.20	0.839	45.45	0.625	66.67	0.800	64.90	0.755
△Gemini1.5-pro	87.37	0.933	93.64	0.967	93.33	0.966	85.57	0.922	94.00	0.969	91.41	0.955
△GPT4o	83.16	0.908	90.91	0.952	92.12	0.959	73.20	0.845	89.33	0.944	86.87	0.930
Model Average (Zero-shot)	64.11	0.759	70.43	0.802	70.31	0.802	54.41	0.680	66.20	0.774	65.87	0.735
◆Swin3D-T*	65.26	0.790	77.27	0.872	83.03	0.907	70.10	0.824	76.67	0.868	75.69	0.862
◆ResNet3D-18*	100.0	1.000	99.09	0.995	98.79	0.994	97.94	0.990	98.67	0.993	98.87	0.994
◆InternVL2.5 (8B)*	100.0	1.000	100.0	1.000	100.0	1.000	100.0	1.000	100.0	1.000	100.0	1.000
◆InternVL3 (9B)*	100.0	1.000	100.0	1.000	100.0	1.000	100.0	1.000	100.0	1.000	100.0	1.000

354 **Figure 4: Deepfake video detection performance comparison of the open-source LMMs. We report**
355 **zero-shot overall accuracy.**

356 and AIGVDet (Bai et al., 2024), which are trained on specific deepfake datasets, show limited zero-
357 shot generalization. The detection models trained on earlier deepfake datasets perform well on
358 known fakes but struggle when exposed to new generative models that are not part of the training
359 data. This limitation arises because these models often learn artifacts specific to the training
360 dataset, leading to poor performance on unseen data. In contrast, LMMs, despite lacking task-
361 specific training for real-fake discrimination, demonstrate relatively robust zero-shot detection per-
362 formance. These models, such as InternLM-XComposer2.5 (7B), show impressive results even
363 without fine-tuning specifically for deepfake detection tasks. However, once fine-tuned for the task,
364 both traditional deep learning-based models and LMMs achieve 100% accuracy on detection tasks.
365 Therefore, the ability to generalize in a zero-shot setting is more critical for deepfake detection, as
366 unseen generative models are constantly evolving.

367 We also launch benchmarks on the real video subsets. From Table 3, we can observe that models
368 exhibit variable performance across different datasets, excelling on more structured datasets such as
369 LIVEVQC and LSVQ but struggling on LIVE-YT-Gaming. This highlights the sensitivity of some
370 models to content type. DeMamba performs the best on real datasets but the worst on AI-generated
371 datasets, indicating that it is biased towards real data and struggle to generalize to AI-generated
372 content. Qwen2.5-VL (7B) and Gemini1.5-pro exhibit high zero-shot accuracy, demonstrating
373 their strong ability to generalize across different real video datasets without any task-specific fine-
374 tuning. Similarly, once fine-tuned for the specific task of deepfake detection, both traditional deep
375 learning models and LMMs achieve near-perfect accuracy, with detection rates approaching 100%.
376 While fine-tuning enhances the performance of traditional deep-learning-based models, LMMs offer
377 greater flexibility, as they are able to perform well without specific task training.

Table 5: Results of cross-generator validation on different training and testing subsets using **Swin3D_T**.

Testing Subset	Training Subset																Avg Acc		
	Alle	Anim	CogV	Hot	LTX	LVDM	LWM	Latt	Lavi	MS	NOVA	T2VZ	Pyra	TAV	VC1	VC2	Wan	ZS	
Allegro	99.3	88.7	7.0	31.3	2.3	0.0	8.7	25.3	37.7	0.7	73.0	59.3	1.3	4.7	0.3	22.0	52.3	0.0	28.6
Animate	74.3	94.0	17.7	43.3	4.3	0.3	28.7	33.7	49.3	1.0	73.7	57.7	1.0	2.3	1.7	17.3	48.0	0.0	30.5
CogVideo	54.0	68.7	96.7	68.7	13.7	0.0	13.3	30.3	69.0	0.7	72.0	45.3	0.0	0.0	4.7	19.0	53.7	3.0	34.0
Hotshot-XL	32.3	42.0	13.7	98.3	5.0	0.3	20.0	37.7	27.0	5.7	86.0	24.7	6.7	5.3	11.0	53.0	27.7	19.7	28.7
LTX	34.0	44.3	6.7	44.7	99.7	0.0	17.3	30.3	42.3	1.7	66.0	28.0	0.7	11.3	6.3	22.7	44.7	2.3	27.9
LVDM	16.0	15.0	0.7	8.0	0.0	99.7	89.3	33.3	43.7	98.7	21.0	8.0	13.3	20.3	50.0	44.3	15.7	0.0	32.1
LWM	29.7	35.3	2.3	38.0	1.7	1.0	99.3	41.3	22.3	18.0	60.0	19.7	4.7	8.7	3.0	25.3	19.3	0.7	23.9
Latte	62.3	63.3	12.7	42.0	6.3	1.7	56.0	81.3	63.7	2.0	73.0	41.7	6.0	17.7	4.7	47.0	52.0	2.0	35.3
Lavie	58.0	66.7	14.0	49.0	8.0	1.0	26.0	44.7	92.7	1.7	74.3	45.7	6.7	8.0	1.3	43.0	58.0	1.7	33.4
ModelScope	7.7	17.0	0.7	50.7	0.0	75.7	95.0	59.3	14.3	99.0	47.0	1.7	2.3	28.0	84.7	54.3	11.0	12.3	36.7
NOVA	70.0	80.7	22.3	87.0	4.3	0.0	21.7	39.3	50.0	0.3	97.7	57.0	1.3	2.0	2.7	43.3	51.7	4.3	35.3
Pyramid	96.0	86.3	15.7	46.7	5.3	0.3	22.7	38.7	80.3	1.3	85.3	98.7	5.3	8.0	1.0	63.3	70.0	0.7	40.3
T2V-Zero	44.3	32.0	0.0	10.3	0.7	0.0	46.3	53.3	75.0	0.3	40.0	36.7	99.3	38.7	1.7	71.7	10.0	0.0	31.1
Tune-A-Video	19.7	18.7	0.3	3.3	1.0	0.0	24.0	45.3	26.3	1.7	8.3	9.0	6.0	88.7	5.0	30.0	20.3	2.3	17.2
VideoCrafer1	15.7	31.0	0.7	69.0	0.0	55.0	19.0	30.3	24.0	86.3	49.3	7.3	2.0	22.7	99.7	75.3	18.7	22.7	34.9
VideoCrafer2	73.0	72.0	8.0	77.0	2.3	1.7	37.7	37.7	78.7	2.0	84.7	60.3	11.3	28.7	10.7	99.3	66.7	5.3	42.1
Wan2.1	79.3	78.7	12.3	38.3	2.0	0.0	8.7	38.7	81.0	1.3	73.3	61.0	0.3	4.7	4.3	44.7	96.3	0.0	34.7
ZeroScope	18.0	43.7	0.7	84.0	1.0	0.0	12.7	18.7	13.3	3.0	51.0	21.3	7.3	27.3	5.7	75.3	13.0	92.0	30.0
ChatGLM	43.3	50.7	11.7	28.0	2.3	0.7	3.0	93	74.3	0.7	60.3	35.3	5.3	3.0	8.3	19.7	35.0	0.7	21.8
Gen3	56.0	61.4	1.6	22.5	0.6	0.0	11.0	22.5	60.6	0.0	54.2	41.8	5.4	11.6	1.6	29.7	36.7	1.2	23.2
Genmo	78.3	55.3	2.0	55.7	0.7	0.0	6.0	24.3	38.7	2.3	73.7	67.0	12.3	4.3	5.7	50.7	41.7	4.3	29.1
Hunyuan	47.7	34.0	3.7	34.0	0.3	0.0	4.3	6.0	31.3	2.3	47.7	35.0	3.0	5.0	3.0	28.7	43.0	0.0	18.3
Hailuo	42.7	30.0	2.0	15.0	0.3	0.0	1.0	4.7	31.0	0.7	25.7	30.7	3.0	7.7	0.3	17.0	38.3	0.3	13.9
Jimeng	38.7	28.7	2.7	29.3	0.3	0.3	2.3	22.3	0.3	28.0	25.7	2.7	3.3	3.7	19.7	29.0	0.0	13.2	
Kling	37.0	35.3	3.3	44.0	2.0	0.0	4.7	6.3	16.7	1.3	60.7	30.3	3.7	10.3	5.3	34.0	31.3	12.3	18.8
Pixverse	57.7	55.3	3.0	49.3	1.7	0.7	11.3	9.3	33.0	1.3	58.7	46.3	2.3	5.0	3.3	46.0	35.7	1.7	23.4
Sora	40.0	40.3	2.7	25.0	0.7	0.0	1.0	10.0	30.0	1.0	29.7	25.3	3.3	13.7	4.3	28.3	37.7	1.7	16.4
VIDUL.5	62.0	48.0	2.7	10.3	0.0	1.0	9.0	6.3	42.7	2.3	37.7	42.3	5.0	3.0	4.3	35.3	41.0	0.0	19.6
Wanxiang	62.7	57.0	3.3	42.7	3.7	0.7	3.3	13.7	25.3	1.3	61.3	46.3	3.3	5.7	1.7	25.7	45.0	0.0	22.4
Xunfei	66.0	58.0	8.3	60.3	0.7	0.7	6.3	12.7	13.0	2.0	65.7	50.3	0.3	1.7	1.3	30.7	36.3	3.7	23.2
Avg Acc	50.5	51.1	9.3	43.5	5.7	8.0	23.6	28.2	43.7	11.4	58.0	38.6	7.5	13.4	13.1	40.5	39.3	6.5	27.3

Table 6: Results of cross-generator validation on different training and testing subsets using **InternVL2.5 (8B)**.

Testing Subset	Training Subset																Avg Acc		
	Alle	Anim	CogV	Hot	LTX	LVDM	LWM	Latt	Lavi	MS	NOVA	T2VZ	Pyra	TAV	VC1	VC2	Wan	ZS	
Allegro	100.0	58.9	44.3	4.7	66.3	0.0	0.0	24.3	8.0	0.0	90.7	83.3	30.1	23.1	4.7	12.7	96.6	19.7	37.1
Animate	46.7	100.0	34.0	55.7	74.7	0.3	7.3	33.7	24.7	0.0	44.0	30.3	3.6	3.4	15.3	52.8	58.8	26.3	34.0
CogVideo	53.3	45.6	100.0	10.0	52.0	0.3	1.3	25.0	35.0	0.0	47.3	42.3	14.4	10.9	34.0	25.0	74.7	40.8	34.0
Hotshot-XL	52.7	58.6	67.0	100.0	95.7	0.0	7.7	64.0	17.7	0.3	34.0	25.0	17.7	24.8	76.3	65.2	80.1	92.8	48.9
LTX	44.7	77.8	26.0	18.3	100.0	0.0	1.3	60.7	4.0	0.0	41.3	27.7	3.6	24.3	53.0	51.5	64.7	67.1	37.0
LVDM	0.0	3.0	0.0	0.0	2.3	100.0	100.0	93.0	0.3	100.0	0.0	0.0	0.0	82.0	27.7	7.0	79.7	1.1	33.7
LWM	3.0	28.3	1.3	0.0	10.0	6.7	100.0	98.7	3.7	38.0	6.7	5.3	17.6	50.0	16.7	30.9	7.2	19.0	
Latte	37.0	69.0	41.3	1.3	57.0	0.0	18.3	100.0	56.0	0.3	42.0	27.3	49.8	83.5	22.7	71.2	68.9	37.6	43.5
Lavie	24.7	70.1	50.0	1.7	20.0	0.7	0.7	86.0	100.0	0.0	47.3	43.7	23.7	14.3	28.0	75.0	74.7	40.1	38.9
ModelScope	2.0	17.6	4.0	5.7	37.7	88.7	100.0	91.7	0.3	100.0	1.0	0.0	22.3	32.1	32.3	60.4	8.8	61.9	37.0
NOVA	70.7	70.5	63.0	15.3	86.7	0.0	0.0	30.7	13.7	0.0	100.0	40.7	3.3	12.7	32.7	52.9	79.7	52.0	37.9
Pyramid	100.0	20.2	72.7	3.3	31.7	0.0	0.0	9.0	31.3	0.0	100.0	100.0	68.9	41.9	9.0	3.9	98.9	18.5	39.4
T2V-Zero	75.7	35.3	18.0	2.0	8.7	1.0	1.3	100.0	89.3	0.0	81.7	79.0	100.0	100.0	9.7	49.3	92.0	29.6	48.5
Tune-A-Video	28.0	8.6	1.0	1.0	8.3	1.0	6.3	99.3	38.0	1.0	30.7	21.7	6.2	63.3	100.0	15.3	53.9	71.9	38.2
VideoCrafer1	0.0	36.7	7.7	4.7	53.0	77.7	0.7	52.7	3.3	61.7	0.0	0.0	0.0	1.3	100.0	96.0	0.7	85.9	30.5
VideoCrafer2	20.7	84.7	32.0	2.0	37.7	0.3	0.3	97.3	88.3	0.0	34.7	26.3	11.6	22.0	74.3	100.0	37.5	86.4	42.0
Wan2.1	79.3	78.7	12.3	38.3	2.0	0.0	8.7	38.7	81.0	1.3	73.3	61.0	1.3	4.7	44.7	100.0	0.0	34.7	29.2
ZeroScope	7.3	61.0	26.0	29.0	78.3	0.0	1.3	11.3	9.0	3.0	3.3	2.0	0.8	10.0	100.0	68.7	14.2	100.0	18.8
ChatGLM	45.3	2.7	54.0	0.3	6.3	0.3	0.0	2.7	10.3	0.0	50.7	43.3	11.6	8.8	5.0	1.7	80.9	13.8	18.8
Gen3	87.3	17.7	26.7	1.0	8.7	0.0	0.3	8.0	21.3	0.0	86.3	81.3	38.8	36.4	7.7	6.5	98.6	18.2	30.3
Genmo	89.0	39.6	63.3	1.7	22.3	0.0	0.0	13.0	17.3	0.0	92.3	86.7	36.3	23.4	12.7	21.0	91.9	44.7	36.4
Hunyuan	25.0	0.0	30.3	0.0	1.0	0.0	0.0	1.0	0.0	0.0	1.7	6.0	0.0	0.8	0.0	0.0	13.3	6.8	4.8
Hailuo	85.3	3.1	29.7	0.7	5.0	0.0	0.0	0.7	2.0	0.0	84.7	75.0	18.6	16.2	3.0	0.0	97.5	14.6	24.2
Jimeng	42.3	0.0	30.3	0.0	0.7	0.0	0.0	0.7	0.3	0.0	26.7	31.0	0.4	13.1	0.0	0.0	65.9	6.9	12.1
Kling	42.0																		

432 4.3 CROSS-GENERATOR VIDEO DETECTION
433

434 From Table 5 and Table 6, we evaluate the per-
435 formance of deepfake detection models trained and
436 evaluated across different video generation models.
437 The detection model is trained on a specific genera-
438 tor and then tested on a variety of other generators.
439 This setup allows us to assess how well the mod-
440 els generalize across different generators, which is
441 crucial for real-world applications where deepfake
442 detection systems may encounter novel generative
443 techniques that are not part of the training data.

444 We train the Swin3D_T and Intern2.5 (8B) on 18
445 open-source video generation models and then eval-
446 uate them on the test set of 30 video generation mod-
447 els, including both open-source and closed-source
448 generators. The results show that models exhibit
449 nearly perfect accuracy close to 100% on genera-
450 tors they have seen during training, as indicated by
451 the bolded diagonal values in the table. This in-
452 dicates that these models are highly specialized in
453 detecting fakes from the specific generator they are
454 trained on. However, the performance significantly
455 drops when the models are tested on generators they
456 haven't encountered before, indicating that while de-
457 tection models can perform exceptionally well on
458 known generative models, their ability to general-
459 ize to new and unseen generative techniques remains
460 limited. This underscores the importance of ensur-
461 ing that deepfake detection systems can generalize
462 effectively, especially as generative models continue
463 to evolve rapidly. It highlights a key challenge for fu-
464 ture research in improving the robustness and adapt-
465 ability of these systems to more advanced video genera-
466 tion models.

467 To further evaluate the generalization ability of our models across diverse generative sources, we
468 train models on a dataset composed of 18 open-source video generation models and tested them on
469 a held-out set of 12 unseen commercial (closed-source) generators. This setting enables a rigorous
470 cross-generator validation, reflecting the model's ability to generalize to previously unseen genera-
471 tive distributions. As shown in Table 7, both Swin3D_T and ResNet3D_18 achieve near-perfect
472 accuracy on the seen open-source generators, indicating strong discriminative capability within the
473 training domain. However, their performance degrades to a certain extent on the unseen commercial
474 generators. These results underscore the importance of model scalability and architectural robust-
475 ness in cross-domain generalization, particularly when handling distribution shifts between training
476 and testing generators.

477 5 CONCLUSION
478

479 In this paper, we present FVBench, a comprehensive benchmark designed to overcome the limita-
480 tions of existing datasets for deepfake video detection. FVBench consists of 120K videos spanning
481 real, AI-edited, and fully AI-generated content, with an emphasis on enhancing both content variety
482 and generative model diversity. We conduct one of the first in-depth studies exploring the potential
483 of LMMs in deepfake video detection. Our results highlight that, while fine-tuned deepfake detec-
484 tion models excel at detecting known fakes, their performance significantly drops when confronted
485 with previously unseen generation models. This underscores the importance of zero-shot general-
486 ization in future detection systems, which is crucial as generative contents continue to become more
487 realistic. We hope FVBench serves as a catalyst for the development of next-generation detection
488 methods and inspires further research into scalable and adaptive content authenticity solutions.

Table 7: Results of cross-generator valida-
tion on 18 open-source generators' training
and 12 unseen generators' testing subsets us-
ing **Swin3D_T** and **ResNet3D_18**. ♡Open-
source lab T2V models. ♠Close-source
commercial T2V models.

Testing models	Training methods		Avg Acc
	Swin3D_T	ResNet3D_18	
♡Allegro	100%	99.7%	99.9%
♡Animate	98.7%	96.0%	97.4%
♡CogVideo	99.3%	100%	99.7%
♡Hotshot-XL	99.3%	99.0%	99.2%
♡LTX	99.7%	98.3%	99.0%
♡LVDM	100%	100%	100%
♡LWM	98.3%	99.0%	98.7%
♡Latte	100%	100%	100%
♡Lavie	99.3%	99.0%	99.2%
♡ModelScope	100%	100%	100%
♡NOVA	100%	100%	100%
♡Pyramid	100%	99.7%	99.9%
♡T2V-Zero	99.3%	100%	99.7%
♡Tune-A-Video	98.7%	97.3%	98.0%
♡VideoCrafer1	100%	100%	100%
♡VideoCrafer2	100%	100%	100%
♡Wan2.1	99.0%	100%	99.5%
♡ZeroScope	100%	100%	100%
♠ChatGLM	98.0%	98.3%	98.2%
♠Gen3	95.2%	96.0%	95.6%
♠Genmo	97.0%	98.7%	97.9%
♠Hunyuan	84.0%	88.3%	86.2%
♠Hailuo	87.3%	89.3%	88.3%
♠Jimeng	71.0%	82.0%	76.5%
♠Kling	87.0%	89.0%	88.0%
♠Pixverse	96.3%	97.7%	97.0%
♠Sora	91.7%	92.3%	92.0%
♠Vidu1.5	90.0%	91.0%	90.5%
♠Wanxiang	93.7%	96.0%	94.9%
♠Xunfei	97.3%	85.0%	91.2%
Avg Acc	96.0%	96.4%	96.2%

486 REFERENCES
487

488 PixVerse AI. Pixverse: Ai video creation platform. <https://pixverse.ai/>, 2024. URL
489 <https://pixverse.ai/>.

490 Jianfa Bai, Man Lin, and Gang Cao. Ai-generated video detection via spatio-temporal anomaly
491 learning. *arXiv preprint arXiv:2403.16638*, 2024.

492 Shuai Bai, Keqin Chen, Xuejing Liu, Jialin Wang, Wenbin Ge, Sibo Song, Kai Dang, Peng Wang,
493 Shijie Wang, Jun Tang, Humen Zhong, Yuanzhi Zhu, Mingkun Yang, Zhaohai Li, Jianqiang Wan,
494 Pengfei Wang, Wei Ding, Zheren Fu, Yiheng Xu, Jiabo Ye, Xi Zhang, Tianbao Xie, Zesen Cheng,
495 Hang Zhang, Zhibo Yang, Haiyang Xu, and Junyang Lin. Qwen2.5-vl technical report. *arXiv*
496 *preprint arXiv:2502.13923*, 2025.

497 Max Bain, Arsha Nagrani, Gü̈l Varol, and Andrew Zisserman. Frozen in time: A joint video and
498 image encoder for end-to-end retrieval. In *Proceedings of the IEEE/CVF International Conference*
499 *on Computer Vision (ICCV)*, pp. 1728–1738, 2021.

500 Duygu Ceylan, Chun-Hao Paul Huang, and Niloy J. Mitra. Pix2video: Video editing using image
501 diffusion. In *Proceedings of the IEEE/CVF International Conference on Computer Vision (ICCV)*,
502 2023. URL <https://arxiv.org/abs/2303.12688>.

503 Haoxin Chen, Menghan Xia, Yingqing He, Yong Zhang, Xiaodong Cun, Shaoshu Yang, Jinbo Xing,
504 Yaofang Liu, Qifeng Chen, Xintao Wang, Chao Weng, and Ying Shan. Videocrafter1: Open
505 diffusion models for high-quality video generation. *arXiv preprint arXiv:2310.19512*, 2023.

506 Haoxin Chen, Yong Zhang, Xiaodong Cun, Menghan Xia, Xintao Wang, Chao Weng, and Ying
507 Shan. Videocrafter2: Overcoming data limitations for high-quality video diffusion models. *arXiv*
508 *preprint arXiv:2401.09047*, 2024a.

509 Haoxing Chen, Yan Hong, Zizheng Huang, Zhuoer Xu, Zhangxuan Gu, Yaohui Li, Jun Lan, Huijia
510 Zhu, Jianfu Zhang, Weiqiang Wang, and Huaxiong Li. Demamba: Ai-generated video detection
511 on million-scale genvideo benchmark, 2024b.

512 Zhe Chen, Weiyun Wang, Yue Cao, Yangzhou Liu, Zhangwei Gao, Erfei Cui, Jinguo Zhu, Shen-
513 glong Ye, Hao Tian, Zhaoyang Liu, et al. Expanding performance boundaries of open-source
514 multimodal models with model, data, and test-time scaling. *arXiv preprint arXiv:2412.05271*,
515 2024c.

516 Zijian Chen, Wei Sun, Yuan Tian, Jun Jia, Zicheng Zhang, Jiarui Wang, Ru Huang, Xiongkuo Min,
517 Guangtao Zhai, and Wenjun Zhang. Gaia: Rethinking action quality assessment for ai-generated
518 videos. In *Proceedings of the Advances in Neural Information Processing Systems (NeurIPS)*,
519 volume 37, pp. 40111–40144, 2024d.

520 Alibaba Cloud. Wanxiang. <https://tongyi.aliyun.com/wanxiang/>, 2024. URL
521 <https://tongyi.aliyun.com/wanxiang/>.

522 Nathaniel Cohen, Vladimir Kulikov, Matan Kleiner, Inbar Huberman-Spiegelglas, and Tomer
523 Michaeli. Slicedit: Zero-shot video editing with text-to-image diffusion models using spatio-
524 temporal slices. In *Proceedings of the International Conference on Machine Learning (ICML)*,
525 pp. 9109–9137, 2024.

526 Yuren Cong et al. Flatten: optical flow-guided attention for consistent text-to-video editing. In
527 *Proceedings of the International Conference on Learning Representations (ICLR)*, 2024. URL
528 <https://openreview.net/forum?id=JgqftqZQZ7>.

529 DeepSeek-AI. Deepseek-r1: Incentivizing reasoning capability in llms via reinforcement learning.
530 *arXiv preprint arXiv:2501.12948*, 2025.

531 Haoge Deng, Ting Pan, Haiwen Diao, Zhengxiong Luo, Yufeng Cui, Huchuan Lu, Shiguang Shan,
532 Yonggang Qi, and Xinlong Wang. Autoregressive video generation without vector quantization.
533 *arXiv preprint arXiv:2412.14169*, 2024.

540 Huiyu Duan, Qiang Hu, Jiarui Wang, Liu Yang, Zitong Xu, Lu Liu, Xiongkuo Min, Chunlei Cai,
 541 Tianxiao Ye, Xiaoyun Zhang, et al. Fineqv: Fine-grained user generated content video qual-
 542 ity assessment. In *Proceedings of the IEEE/CVF Conference on Computer Vision and Pattern*
 543 *Recognition (CVPR)*, 2025.

544 Hichem Felouat, Huy H Nguyen, Trung-Nghia Le, Junichi Yamagishi, and Isao Echizen. ekyc-df:
 545 A large-scale deepfake dataset for developing and evaluating ekyc systems. *IEEE Access*, 12:
 546 30876–30892, 2024.

548 Ruoyu Feng, Wenming Weng, Yanhui Wang, Yuhui Yuan, Jianmin Bao, Chong Luo, Zhibo Chen,
 549 and Baining Guo. Ccredit: Creative and controllable video editing via diffusion models. In *Pro-
 550 ceedings of the IEEE/CVF Conference on Computer Vision and Pattern Recognition (CVPR)*, pp.
 551 6712–6722, 2024.

552 Team GLM et al. Chatglm: A family of large language models from glm-130b to glm-4 all tools.
 553 *arXiv preprint arXiv:2406.12793*, 2024.

555 Daya Guo, Dejian Yang, Huawei Zhang, Junxiao Song, Ruoyu Zhang, Runxin Xu, Qihao Zhu,
 556 Shirong Ma, Peiyi Wang, Xiao Bi, et al. Deepseek-r1: Incentivizing reasoning capability in llms
 557 via reinforcement learning. *arXiv preprint arXiv:2501.12948*, 2025.

558 Yoav HaCohen, Nisan Chiprut, Benny Brazowski, Daniel Shalem, Dudu Moshe, Eitan Richardson,
 559 Eran Levin, Guy Shiran, Nir Zabari, Ori Gordon, Poriya Panet, Sapir Weissbuch, Victor Kulikov,
 560 Yaki Bitterman, Zeev Melumian, and Ofir Bibi. Ltx-video: Realtime video latent diffusion. *arXiv*
 561 *preprint arXiv:2501.00103*, 2024.

562 Yingqing He, Tianyu Yang, Yong Zhang, Ying Shan, and Qifeng Chen. Latent video diffusion
 563 models for high-fidelity long video generation. *arXiv preprint arXiv:2211.13221*, 2022.

565 Vlad Hosu, Franz Hahn, Mohsen Jenadeleh, Hanhe Lin, Hui Men, Tamás Szirányi, Shujun Li, and
 566 Dietmar Saupe. The konstanz natural video database (konvid-1k). In *Proceedings of the IEEE*
 567 *International Conference on Quality of Multimedia Experience (QoMEX)*, pp. 1–6, 2017.

568 Yang Hou, Zhaoyu Zhang, Zhaoxu Yang, Teng Wang, Qiong Liu, and Guang Han. Polyglotfake: A
 569 novel multilingual and multimodal deepfake dataset. *arXiv preprint arXiv:2405.08838*, 2024.

571 Edward J Hu et al. Lora: Low-rank adaptation of large language models. In *Proceedings of the*
 572 *International Conference on Learning Representations (ICLR)*, volume 1, pp. 3, 2022.

574 Yang Jin, Zhicheng Sun, Ningyuan Li, Kun Xu, Kun Xu, Hao Jiang, Nan Zhuang, Quzhe Huang,
 575 Yang Song, Yadong Mu, and Zhouchen Lin. Pyramidal flow matching for efficient video genera-
 576 tive modeling. *arXiv preprint arXiv:2410.05954*, 2024.

577 Ozgur Kara, Bariscan Kurtkaya, Hidir Yesiltepe, James M. Rehg, and Pinar Yanardag. Rave: Ran-
 578 domized noise shuffling for fast and consistent video editing with diffusion models. In *Pro-
 579 ceedings of the IEEE/CVF Conference on Computer Vision and Pattern Recognition (CVPR)*, pp.
 580 6507–6516, 2024.

581 Will Kay, Joao Carreira, Karen Simonyan, Brian Zhang, Chloe Hillier, Sudheendra Vijaya-
 582 narasimhan, Fabio Viola, Tim Green, Trevor Back, Paul Natsev, Mustafa Suleyman, and Andrew
 583 Zisserman. The kinetics human action video dataset. *arXiv preprint arXiv:1705.06950*, 2017.

585 Levon Khachatryan, Andranik Mousisyan, Vahram Tadevosyan, Roberto Henschel, Zhangyang
 586 Wang, Shant Navasardyan, and Humphrey Shi. Text2video-zero: Text-to-image diffusion models
 587 are zero-shot video generators. *arXiv preprint arXiv:2303.13439*, 2023.

588 Hasam Khalid, Shahroz Tariq, Minha Kim, and Simon S Woo. Fakeavceleb: A novel audio-video
 589 multimodal deepfake dataset. In *Conference on Neural Information Processing Systems Datasets*
 590 *and Benchmarks Track*, 2021.

592 Kartik Kuckreja et al. Indiface: Illuminating india’s deepfake landscape with a comprehensive
 593 synthetic dataset. In *International Conference on Automatic Face and Gesture Recognition*, pp.
 1–8, 2024.

594 Bo Li, Yuanhan Zhang, Dong Guo, Renrui Zhang, Feng Li, Hao Zhang, Kaichen Zhang, Peiyuan
 595 Zhang, Yanwei Li, Ziwei Liu, and Chunyuan Li. Llava-onevision: Easy visual task transfer. *arXiv*
 596 *preprint arXiv:2408.03326*, 2024a.

597

598 Feng Li, Renrui Zhang, Hao Zhang, Yuanhan Zhang, Bo Li, Wei Li, Zejun Ma, and Chunyuan Li.
 599 Llava-next-interleave: Tackling multi-image, video, and 3d in large multimodal models. *arXiv*
 600 *preprint arXiv:2407.07895*, 2024b.

601

602 Zhimin Li, Jianwei Zhang, Qin Lin, Jiangfeng Xiong, Yanxin Long, Xinchi Deng, Yingfang Zhang,
 603 Xingchao Liu, Minbin Huang, Zedong Xiao, et al. Hunyuan-dit: A powerful multi-resolution
 604 diffusion transformer with fine-grained chinese understanding. *arXiv preprint arXiv:2405.08748*,
 605 2024c.

606

607 Hao Liu, Wilson Yan, Matei Zaharia, and Pieter Abbeel. World model on million-length video and
 608 language with blockwise ringattention. *arXiv preprint arXiv:2402.08268*, 2024a.

609

610 Haotian Liu, Chunyuan Li, Yuheng Li, and Yong Jae Lee. Improved baselines with visual instruction
 611 tuning. In *Proceedings of the IEEE/CVF Conference on Computer Vision and Pattern Recognition*
 612 (*CVPR*), pp. 26296–26306, 2024b.

613

614 Xin Ma et al. Latte: Latent diffusion transformer for video generation. *Transactions on Machine
 615 Learning Research*, 2025.

616

617 AI Meta. Llama 3.2: Revolutionizing edge ai and vision with open, customizable models. *Meta AI
 618 Blog. Retrieved December*, 20:2024, 2024.

619

620 Trisha Mittal, Ritwik Sinha, Viswanathan Swaminathan, John Collomosse, and Dinesh Manocha.
 621 Video manipulations beyond faces: A dataset with human-machine analysis. *arXiv preprint
 622 arXiv:2207.13064*, 2022.

623

624 John Mullan, Duncan Crawbuck, and Aakash Sastry. Hotshot-XL. <https://github.com/hotshotco/hotshot-xl>, 2023. URL <https://github.com/hotshotco/hotshot-xl>.

625

626 Jordi Pont-Tuset, Federico Perazzi, Sergi Caelles, Pablo Arbeláez, Alex Sorkine-Hornung, and
 627 Luc Van Gool. The 2017 davis challenge on video object segmentation. *arXiv preprint
 628 arXiv:1704.00675*, 2018.

629

630 Chenyang Qi, Xiaodong Cun, Yong Zhang, Chenyang Lei, Xintao Wang, Ying Shan, and Qifeng
 631 Chen. Fatezero: Fusing attentions for zero-shot text-based video editing. In *Proceedings of
 632 the IEEE/CVF International Conference on Computer Vision (ICCV)*, 2023. URL <https://arxiv.org/abs/2303.09535>.

633

634 Liao Qu, Huichao Zhang, Yiheng Liu, Xu Wang, Yi Jiang, Yiming Gao, Hu Ye, Daniel K. Du, Ze-
 635 huan Yuan, and Xinglong Wu. Tokenflow: Unified image tokenizer for multimodal understand-
 636 ing and generation. In *Proceedings of the International Conference on Learning Representations*
 637 (*ICLR*), 2023.

638

639 Andreas Rossler et al. Faceforensics++: Learning to detect manipulated facial images. In *Proceed-
 640 ings of the IEEE/CVF international conference on computer vision (ICCV)*, pp. 1–11, 2019.

641

642 Runway. Introducing gen-3 alpha: A new frontier for video generation. <https://runwayml.com/research/introducing-gen-3-alpha>, 2024. URL <https://runwayml.com/research/introducing-gen-3-alpha>.

643

644 Zeina Sinno and Alan Conrad Bovik. Large-scale study of perceptual video quality. *IEEE Transac-
 645 tions on Image Processing (TIP)*, 28(2):612–627, 2018.

646

647 ByteDance Team. Jimeng ai. <https://jimeng.jianying.com/>, 2024a. URL <https://jimeng.jianying.com/>.

648

649 Genmo Team. Gemo. <https://www.genmo.ai>, 2024b. URL <https://www.genmo.ai>.

650

651 Kuaishou Team. Kling ai. <https://klingai.io/>, 2024c. URL <https://klingai.io/>.

648 MiniMax Team. Hailuo ai. <https://hailuoai.video/>, 2024d. URL <https://hailuoai.video/>.

649

650

651 OpenAI Team. Sora. <https://openai.com/research/video-generation-models-as-world-simulators>, 2024e. URL <https://openai.com/research/video-generation-models-as-world-simulators>.

652

653

654 Vidu AI Team. Vidu ai. <https://www.vidu.studio/zh>, 2024f. URL <https://www.vidu.studio/zh>.

655

656

657 Xunfei Team. Xunfei. <https://typemovie.art/>, 2024g. URL <https://typemovie.art/>.

658

659 Zeroscope Team. Zeroscope. https://huggingface.co/cerspense/zeroscope_v2_XL, 2024h. URL https://huggingface.co/cerspense/zeroscope_v2_XL.

660

661

662 Ang Wang et al. Wan: Open and advanced large-scale video generative models. *arXiv preprint arXiv:2503.20314*, 2025a.

663

664 Jiarui Wang, Huiyu Duan, Ziheng Jia, Yu Zhao, Woo Yi Yang, Zicheng Zhang, Zijian Chen, Junlong Wang, Yuke Xing, Guangtao Zhai, and Xiongkuo Min. Love: Benchmarking and evaluating text-to-video generation and video-to-text interpretation. *arXiv preprint arXiv:2505.12098*, 2025b.

665

666

667 Jiarui Wang, Huiyu Duan, Junlong Wang, Ziheng Jia, Woo Yi Yang, Xiaorong Zhu, Yu Zhao, Jiaying Qian, Yuke Xing, Guangtao Zhai, and Xiongkuo Min. Dfbench: Benchmarking deepfake image detection capability of large multimodal models. *arXiv preprint arXiv:2506.03007*, 2025c.

668

669

670

671 Jiarui Wang, Huiyu Duan, Guangtao Zhai, Junlong Wang, and Xiongkuo Min. Aigv-assessor: Benchmarking and evaluating the perceptual quality of text-to-video generation with lmm. In *Proceedings of the IEEE/CVF Conference on Computer Vision and Pattern Recognition (CVPR)*, 2025d.

672

673

674

675 Jiarui Wang, Huiyu Duan, Yu Zhao, Junlong Wang, Guangtao Zhai, and Xiongkuo Min. Lmm4lmm: Benchmarking and evaluating large-multimodal image generation with lmms. *arXiv preprint arXiv:2504.08358*, 2025e.

676

677

678 Jiniu Wang et al. Modelscope text-to-video technical report. *arXiv preprint arXiv:2308.06571*, 2023a.

679

680

681 Wen Wang et al. Zero-shot video editing using off-the-shelf image diffusion models. *arXiv preprint arXiv:2303.17599*, 2024.

682

683

684 Yaohui Wang et al. Lavie: High-quality video generation with cascaded latent diffusion models. *arXiv preprint arXiv:2309.15103*, 2023b.

685

686 Yilin Wang et al. Youtube ugc dataset for video compression research. In *Proceedings of the IEEE International Workshop on Multimedia Signal Processing (MMSP)*, pp. 1–5, 2019.

687

688

689 Jay Zhangjie Wu et al. Tune-a-video: One-shot tuning of image diffusion models for text-to-video generation. In *Proceedings of the IEEE/CVF International Conference on Computer Vision (ICCV)*, pp. 7623–7633, 2023.

690

691

692 Liangbin Xie et al. Vfqhq: A high-quality dataset and benchmark for video face super-resolution. In *Proceedings of the IEEE/CVF conference on computer vision and pattern recognition*, pp. 20110–20119, 2022.

693

694

695 Jiaqi Xu et al. Easyanimate: A high-performance long video generation method based on transformer architecture. *arXiv preprint arXiv:2405.18991*, 2024.

696

697

698 Jun Xu, Tao Mei, Ting Yao, and Yong Rui. Msr-vtt: A large video description dataset for bridging video and language. In *Proceedings of the IEEE/CVF Conference on Computer Vision and Pattern Recognition (CVPR)*, 2016.

699

700 URL <https://www.microsoft.com/en-us/research/publication/msr-vtt-a-large-video-description-dataset-for-bridging-video-and-language/>.

701

702 Zitong Xu, Huiyu Duan, Bingnan Liu, Guangji Ma, Jiarui Wang, Liu Yang, Shiqi Gao, Xiaoyu
 703 Wang, Jia Wang, Xiongkuo Min, Guangtao Zhai, and Weisi Lin. Lmm4edit: Benchmarking and
 704 evaluating multimodal image editing with lmms. *arXiv preprint arXiv:2507.16193*, 2025.

705

706 Zhiyuan Yan et al. Df40: Toward next-generation deepfake detection. In *Conference on Neu-
 707 ral Information Processing Systems Datasets and Benchmarks Track*, 2024. URL <https://openreview.net/forum?id=rtkpcN3S24>.

708

709 Shuai Yang, Yifan Zhou, Ziwei Liu, and Chen Change Loy. Fresco: Spatial-temporal correspon-
 710 dence for zero-shot video translation. In *Proceedings of the IEEE/CVF Conference on Computer
 711 Vision and Pattern Recognition (CVPR)*, 2024a. URL <https://arxiv.org/abs/2403.12962>.

712

713

714 Woo Yi Yang, Jiarui Wang, Sijing Wu, Huiyu Duan, Yuxin Zhu, Liu Yang, Kang Fu, Guangtao
 715 Zhai, and Xiongkuo Min. Lmme3dhf: Benchmarking and evaluating multimodal 3d human face
 716 generation with lmms. *arXiv preprint arXiv:2504.20466*, 2025.

717

718 Xin Yang, Yuezun Li, and Siwei Lyu. Exposing deep fakes using inconsistent head poses. In
 719 *ICASSP 2019-2019 IEEE International Conference on Acoustics, Speech and Signal Processing
 (ICASSP)*, pp. 8261–8265. IEEE, 2019.

720

721 Zhuoyi Yang, Jiayan Teng, Wendi Zheng, Ming Ding, Shiyu Huang, Jiazheng Xu, Yuanming Yang,
 722 Wenyi Hong, Xiaohan Zhang, Guanyu Feng, et al. Cogvideox: Text-to-video diffusion models
 723 with an expert transformer. *arXiv preprint arXiv:2408.06072*, 2024b.

724

725 Yuan Yao, Tianyu Yu, Ao Zhang, Chongyi Wang, Junbo Cui, Hongji Zhu, Tianchi Cai, Haoyu Li,
 726 Weilin Zhao, Zihui He, et al. Minicpm-v: A gpt-4v level mllm on your phone. *arXiv preprint
 727 arXiv:2408.01800*, 2024.

728

729 Jiabo Ye, Haiyang Xu, Haowei Liu, Anwen Hu, Ming Yan, Qi Qian, Ji Zhang, Fei Huang, and
 730 Jingren Zhou.mplug-owl3: Towards long image-sequence understanding in multi-modal large
 731 language models. In *Proceedings of the International Conference on Learning Representations
 (ICLR)*, 2024.

732

733 Zhenqiang Ying, Maniratnam Mandal, Deepti Ghadiyaram, and Alan Bovik. Patch-vq: patching
 734 up the video quality problem. In *Proceedings of the IEEE Conference on Computer Vision and
 735 Pattern Recognition (CVPR)*, pp. 14019–14029, 2021.

736

737 Xiangxu Yu, Zhenqiang Ying, Neil Birkbeck, Yilin Wang, Balu Adsumilli, and Alan C Bovik. Sub-
 738 jective and objective analysis of streamed gaming videos. *IEEE Transactions on Games*, 2023.

739

740 Haoyu Zhang, Kaihao Wang, Yifei Chen, Hang Zhou, Zhipeng Wei, and Lin gun Wu. Fakehuman-
 741 vid: A large-scale fine-grained video deepfake dataset. *arXiv preprint arXiv:2405.10545*, 2024a.

742

743 Pan Zhang, Xiaoyi Dong, Yuhang Zang, Yuhang Cao, Rui Qian, Lin Chen, Qipeng Guo, Haodong
 744 Duan, Bin Wang, Linke Ouyang, Songyang Zhang, Wenwei Zhang, Yining Li, Yang Gao, Peng
 745 Sun, Xinyue Zhang, Wei Li, Jingwen Li, Wenhui Wang, Hang Yan, Conghui He, Xingcheng
 746 Zhang, Kai Chen, Jifeng Dai, Yu Qiao, Dahua Lin, and Jiaqi Wang. Internlm-xcomposer-2.5: A
 747 versatile large vision language model supporting long-contextual input and output. *arXiv preprint
 748 arXiv:2407.03320*, 2024b.

749

750 Yabo Zhang, Yuxiang Wei, Dongsheng Jiang, Xiaopeng Zhang, Wangmeng Zuo, and Qi Tian. Con-
 751 trolvideo: Training-free controllable text-to-video generation. In *Proceedings of the International
 752 Conference on Learning Representations (ICLR)*, 2024c. URL <https://openreview.net/forum?id=5a79AqFr0c>.

753

754 Zhonghao Zhang et al. Ivy-fake: A unified explainable framework and benchmark for image and
 755 video aigc detection. *arXiv preprint arXiv:2406.00979*, 2024d.

756

757 Yuan Zhou, Qiuyue Wang, Yuxuan Cai, and Huan Yang. Allegro: Open the black box of
 758 commercial-level video generation model. *arXiv preprint arXiv:2410.15458*, 2024.

756 **A APPENDIX**
757758 We clarify the use of LLM in section B, the detail information of T2V models in section C, de-
759 tail information of the LMMs in section D, more result comparisons in section E and the training
760 hyperparameters in section F.
761762 **B USE OF LLM**
763764 During the drafting of this manuscript, LLM (GPT4o) was employed to enhance the text’s fluency,
765 rectify grammatical inaccuracies, and improve the precision of phrasing. However, the central ideas,
766 experimental design, and final conclusions are generated without AI contribution.
767768 **C DETAILED INFORMATION OF T2V MODELS**
769770 **Pyramid** Jin et al. (2024) introduces a novel pyramidal flow matching strategy for video generation,
771 which progressively aligns data distributions at multiple scales. This enables high-quality synthesis
772 while potentially reducing computational demand.
773774 **Wan2.1** Wang et al. (2025a) is an open-source large-scale video generation model developed under
775 the “Wan” initiative. It is optimized for high-fidelity video creation and aims to enhance accessibility
776 and transparency in advanced generative AI research.
777778 **Allegro** Zhou et al. (2024) aims to replicate commercial-grade video synthesis within a transparent
779 framework. Its goal is to demystify the “black box” nature of high-end video models while striving
780 for comparable visual quality.
781782 **VideoCrafter2** Chen et al. (2024a) addresses the lack of high-quality video training data by sepa-
783 rating motion and appearance at the data level. It utilizes low-resolution videos for learning motion
784 and high-quality images for preserving appearance.
785786 **CogVideo X1.5** Yang et al. (2024b) is a diffusion-based text-to-video model featuring an Expert
787 Transformer, designed to improve efficiency, scalability, and specialization in complex video syn-
788 thesis.
789790 **Animate** Xu et al. (2024) proposes a transformer-based method for generating long-form videos
791 with temporal consistency, focusing on modeling long-range dependencies to preserve narrative
792 coherence.
793794 **Lavie** Wang et al. (2023b) adopts a cascaded latent diffusion architecture, generating and refining
795 video content in stages within the latent space. This design improves detail and coherence in high-
796 resolution video generation.
797798 **Hotshot-XL** Mullan et al. (2023) is a text-to-GIF model adapted for video output by converting
799 GIFs to MP4 format. It is built on Stable Diffusion XL and employs default settings from its official
800 implementation.
801802 **Latte** Ma et al. (2025) is a latent diffusion video model based on a Transformer backbone. It encodes
803 videos via a pretrained VAE and processes spatial-temporal tokens using four architectural variants
804 for efficient and expressive synthesis.
805806 **VideoCrafter1** Chen et al. (2023) presents two diffusion models: one for text-to-video and an-
807 other for image-to-video generation. By incorporating temporal attention, it enhances consistency
808 in videos generated from large-scale datasets.
809810 **NOVA** Deng et al. (2024) reframes video generation as an autoregressive prediction task across time
811 and space. This design allows efficient frame-by-frame synthesis and supports flexible, zero-shot
812 generative capabilities.
813814 **ModelScope** Wang et al. (2023a) proposes a decomposed diffusion approach that separates base
815 and residual noise across frames. This improves spatial-temporal consistency while benefiting from
816 pretrained generative modules.
817

810 **Text2Video-Zero** Khachatryan et al. (2023) is a zero-shot text-to-video model that requires no fine-
 811 tuning. It introduces motion dynamics between latent codes and uses cross-frame attention to ensure
 812 temporal coherence.

813 **Tune-A-Video** Wu et al. (2023) is a one-shot text-to-video generation model employing sparse
 814 spatio-temporal attention. It can generate coherent videos from a single example and supports con-
 815 ditional or personalized inputs.

816 **LTX** HaCohen et al. (2024) is a real-time video generation model based on latent diffusion. Its key
 817 strength lies in reducing generation latency, allowing interactive video synthesis without compro-
 818 mising quality.

819 **LVDM** He et al. (2022) leverages a hierarchical diffusion design in latent space to extend generation
 820 length and reduce computational cost. It includes conditional perturbation and guidance to maintain
 821 quality across extended durations.

822 **ZeroScope** Team (2024h) serves as a specialized upscaler for outputs generated with zero-
 823 scope_v2_576w. By converting low-resolution previews to high-resolution videos, it enables faster
 824 iteration with high visual fidelity.

825 **LWM** Liu et al. (2024a) is a multimodal autoregressive model that uses RingAttention to handle
 826 long sequences efficiently. It supports strong video-language understanding and generation with a
 827 context window of up to 1M tokens.

828 **Pixverse** AI (2024) is an all-in-one AI video tool that supports viral effects, video-to-video restyling,
 829 lip-sync, and AI-based video extension. It's beginner-friendly yet powerful enough for advanced
 830 users, making it ideal for both casual and professional video creation.

831 **Wanxiang** Cloud (2024), developed by Alibaba DAMO Academy, is a multimodal large model
 832 capable of cross-modal generation and understanding across text, video, and audio. It supports tasks
 833 such as text-to-video and visual question answering.

834 **Hailuo** Team (2024d), by MiniMax, enables text-to-video and video editing through simple prompts.
 835 It offers an accessible platform for generating high-quality videos in marketing, education, and
 836 entertainment.

837 **Jimeng** Team (2024a), from Faceu Technology, is a text-to-video model focused on generating
 838 short, realistic video clips with precise prompt interpretation.

839 **Sora** Team (2024e) excels in prompt understanding, generating emotionally expressive characters,
 840 multi-shot videos, and complex scenes with consistent motion and detail.

841 **Hunyuan** Li et al. (2024c) is a 13B-parameter open-source text-to-video model that produces videos
 842 with strong physical realism and scene consistency, supporting creative visual generation.

843 **Vidu 1.5** Team (2024f) introduces Multiple-Entity Consistency, allowing unrelated characters, ob-
 844 jects, and environments to be seamlessly combined into visually coherent videos, even with complex
 845 inputs.

846 **Gen3** Runway (2024) marks a new generation of foundation models from Runway, built on a fresh
 847 large-scale multimodal training infrastructure. Trained jointly on video data, Gen-3 Alpha powers a
 848 range of tools including text-to-video, video-to-video, and motion editing modes like motion brush
 849 and director mode, while also supporting upcoming features for finer control over structure, style,
 850 and motion.

851 **Kling** Team (2024c), developed by Kuaishou's Large Model Algorithm Team, represents a new
 852 class of AI creativity tools, offering rich capabilities for generating and editing AI-generated video
 853 content with high controllability.

854 **Genmo** Team (2024b) is an AI creation assistant designed for video generation and editing. Users
 855 can create animations and stylized videos from text or images, as well as restyle existing footage,
 856 making it a versatile platform for creative exploration.

857 **ChatGLM** GLM et al. (2024), from Zhipu AI and Tsinghua University's KEG lab, is a bilingual
 858 large language model family ranging from GLM-130B to the advanced GLM-4. The latest ver-
 859 860 861 862 863

864
 865 **Table 8: An overview and URLs of the adopted 30 T2V generation models.** ♦Open-source lab T2V
 866 models. ♠Close-source commercial T2V models. †Representative variable and optional.

Models	Frames	FPS	Resolution	URL
♦Pyramid Jin et al. (2024)	121	24	1280×768	https://github.com/jy0205/Pyramid-Flow
♦Wan2.1 Wang et al. (2025a)	81 [†]	16 [†]	832×480 [†]	https://github.com/FoundationVision/LlamaGen
♦Allegro Zhou et al. (2024)	88	15	1280×720	https://github.com/rhymes-ai/Allegro
♦VideoCrafter2 Chen et al. (2024a)	16	10	512×320	https://github.com/AILab-CVC/VideoCrafter
♦CogVideo X1.5 Yang et al. (2024b)	32	8	1360×768	https://github.com/THUDM/CogVideo
♦Animate Xu et al. (2024)	49	8	672×384	https://github.com/aigc-apps/EasyAnimate
♦Lavie Wang et al. (2023b)	16	8	512×320	https://github.com/Vchitect/LaVie
♦Hotshot-XL Mullan et al. (2023)	8	8	672×384	https://github.com/hotshotco/Hotshot-XL
♦Latte Ma et al. (2025)	16	8	512×512	https://github.com/Vchitect/Latte
♦VideoCrafter1 Chen et al. (2023)	16 [†]	10 [†]	512×320 [†]	https://github.com/AILab-CVC/VideoCrafter
♦Text2Video-Zero Khachaturyan et al. (2023)	8	4	512×512	https://github.com/Picsart-AI-Research/Text2Video-Zero
♦NOVA Deng et al. (2024)	33	12	768×480	https://github.com/baaivision/NOVA
♦ModelScope Wang et al. (2023a)	16	8	256×256	https://github.com/modelscope/modelscope
♦Tune-A-Video Wu et al. (2023)	8	8	512×512	https://github.com/showlab/Tune-A-Video
♦LTX HaCohen et al. (2024)	121	25	704×480	https://github.com/Lighttricks/LTX-Video
♦LVDM He et al. (2022)	16	8	256×256	https://github.com/YingqingHe/LVDM
♦ZeroScope Team (2024h)	36	8	576×320	https://huggingface.co/cerspense/zeroscope_v2_XL
♦LWM Liu et al. (2024a)	8	4	256×256	https://github.com/LargeWorldModel/LWM
♦Pixverse AI (2024)	161 [†]	30 [†]	640×360 [†]	https://pixverse.ai/
♠Wanxiang Cloud (2024)	161 [†]	30 [†]	1280×720 [†]	https://tongyi.aliyun.com/wanxiang/
♠Hailuo Team (2024d)	141 [†]	25 [†]	1280×720 [†]	https://hailucai.video/
♠Jimeng Team (2024a)	12 [†] 1	24 [†]	1472×832 [†]	https://jimeng.jianying.com/
♠Sora Team (2024e)	150 [†]	30 [†]	854×480 [†]	https://openai.com/research/video-generation-models-as-world-simulators
♠Hunyuan Li et al. (2024c)	129 [†]	24 [†]	1280×720 [†]	https://aivideo.hunyuan.tencent.com/
♠Vidul.5 Team (2024f)	60 [†]	16 [†]	688×384 [†]	https://www.vidul.studio/zh
♠Gen3 Runway (2024)	128 [†]	24 [†]	1280×768 [†]	https://runwayml.com/research/introducing-gen-3-alpha
♠Kling Team (2024c)	153 [†]	30 [†]	1280×720 [†]	https://klingai.io/
♠Genmo Team (2024b)	60 [†]	15 [†]	1728×1728 [†]	https://www.genmo.ai
♠ChatGLM GLM et al. (2024)	151 [†]	30 [†]	1280×720 [†]	https://chatglm.cn/video?lang=zh
♠Xunfei Team (2024g)	145 [†]	24 [†]	1024×576 [†]	https://typemovie.art/

888
 889 sion integrates an “All Tools” framework, enabling enhanced interaction with external modules for
 890 complex tasks.

891 **Xunfei Team (2024g)**, by iFlytek, offers an AI-driven platform for quickly turning text into video.
 892 It simplifies video creation by providing a variety of styles and templates suited for producing short-
 893 form visual content efficiently.

894 D DETAILED INFORMATION OF THE LMMS

895 **LLaVA-NeXT-Video** Li et al. (2024b) boosts video input resolution and enhances fine-grained per-
 896 ception capabilities, including OCR, visual reasoning, and factual knowledge grounding. It retains
 897 a compact training setup, relying on fewer than one million instruction-tuning samples to achieve
 898 high efficiency and broad generalization.

902 **VideoLLaVA** Liu et al. (2024b) presents a unified framework that bridges visual input with language
 903 representations by aligning visual features before projecting them into the language space. This
 904 approach empowers large language models to jointly reason over both images and video content
 905 within a shared architecture.

906 **InternVL2.5** Chen et al. (2024c) demonstrates strong multimodal capabilities across benchmarks
 907 involving cross-domain reasoning, document comprehension, and video analysis. It benefits from
 908 enhanced vision encoders, a larger training corpus, and optimized inference strategies, resulting in
 909 improved generalization and hallucination mitigation.

911 **InternVL3** Chen et al. (2024c) pushes the boundaries of multimodal LLMs by supporting a wider
 912 range of applications, including tool use, GUI interaction, industrial visual tasks, and 3D scene
 913 understanding. By unifying vision-language learning into a single-stage framework, it eliminates
 914 the need for additional adapters or fusion modules, streamlining training and improving scalability.

915 **VideoLlama3** Yao et al. (2024) adopts a four-stage training pipeline for vision-language modeling.
 916 It introduces innovations such as Rotary Position Embedding (RoPE) for adaptive image resolution
 917 handling and video token compression for efficient temporal representation, yielding strong per-
 918 formance across visual understanding tasks in both image and video modalities.

918
 919 **Table 9: Performance benchmark on AI-generated video subsets as a supplement to the Table**
 920 **2 in the main paper.** ♦* refers to finetuned models.

Methods / Datasets	Genmo	Hailuo	T2V-Zero	Tune-A-Video	LVDM	LWM	LTX	ZeroScope	Jimeng	VCrafter2	
♦AIGVDet*	100.0%	100.0%	100.0%	100.0%	96.43%	93.12%	100.0%	100.0%	100.0%	100.0%	
♦MC3_18*	100.0%	100.0%	100.0%	100.0%	100.0%	100.0%	100.0%	100.0%	100.0%	100.0%	
Methods / Datasets	Xunfei	Hotshot	Hunyuan	CogVideo	NOVA	VCrafter1	Sora	ChatGLM	Wan2.1	Animate	
♦AIGVDet*	100.0%	100.0%	100.0%	100.0%	100.0%	100.0%	100.0%	100.0%	100.0%	100.0%	
♦MC3_18*	100.0%	100.0%	100.0%	100.0%	100.0%	100.0%	100.0%	100.0%	100.0%	100.0%	
Methods / Datasets	Wanxiang	Allegro	Pyramid	Vidu1.5	Lavie	Kling	Pixverse	Latte	MScope	Gen3	Overall
♦AIGVDet*	100.0%	100.0%	98.24%	100.0%	100.0%	100.0%	100.0%	100.0%	100.0%	100.0%	99.59%
♦MC3_18*	100.0%	100.0%	100.0%	100.0%	100.0%	100.0%	100.0%	100.0%	100.0%	100.0%	100.0%

930 **Table 10: Performance benchmark on real video subsets as a supplement to the Table 3 in the**
 931 **main paper.** ♦* refers to model zero-shot results. ♦* refers to finetuned models.

Methods / Datasets	MSRVTT	KoNViD	FineVD	WebVid	LSVQ	LIVEVQC	YouTubeUGC	LIVE-YT-Gaming	Overall
♦MM-Det	0.20%	2.08%	3.59%	4.51%	7.25%	13.68%	0.44%	0.0%	3.97%
♦AIGVDet*	99.43%	97.81%	98.32%	100.0%	96.89%	99.42%	100.0%	99.17%	98.88%
♦MC3_18*	99.75%	99.48%	98.77%	99.67%	97.56%	97.85%	100.0%	100.0%	98.91%

937 **LLaMA3.2-Vision** Meta (2024) excels in video-based reasoning tasks, including understanding
 938 complex documents, interpreting data visualizations, and performing visual grounding. The model
 939 is capable of interpreting structured content such as charts and maps, while generating descriptive
 940 and context-aware captions for visual inputs.

941 **mPLUG-Owl3** Ye et al. (2024) is a robust multimodal model designed for understanding extended
 942 video sequences and interleaved video-text content. It features a novel Hyper Attention mechanism
 943 that fuses visual and textual signals into a shared embedding space, enabling effective processing of
 944 long-form and multi-video inputs.

945 **Qwen2.5-VL** Bai et al. (2025) represents the latest evolution of the Qwen vision-language family.
 946 It enhances recognition and localization capabilities, supports document-level reasoning, and im-
 947 proves long-video understanding through dynamic resolution scaling, absolute temporal encoding,
 948 and optimized inference via window-based attention mechanisms.

950 **LLaVA-One-Vision** Li et al. (2024a) is an open-source multimodal model designed for scalable
 951 visual-language learning across single images, image sequences, and video data. It features a cost-
 952 efficient architecture that links vision encoders with language models, enabling effective knowledge
 953 transfer from image to video tasks.

954 **InternLM-XComposer-2.5** Zhang et al. (2024b) is a powerful vision-language model built on
 955 InternLM2-7B, supporting long-context inputs up to 96K tokens. It also enables webpage gener-
 956 ation and text-image article composition. It offers a strong open-source alternative for both vision-
 957 language understanding and content generation.

959 E MORE RESULT COMPARISONS

961 To further support the results presented in the main paper, we extend the experiments in the original
 962 tables by including additional models for training and evaluation, as shown in Tables 9- 12.

964 F TRAINING HYPERPARAMETERS

966 The following hyperparameters were consistently used across the training stages:

- 968 • **Dataset Split:** The dataset was partitioned into training and testing sets using a 4:1 ratio.
- 969 • **Learning Rate:** 4×10^{-5} (i.e., 4×10^{-5}).
- 970 • **Batch Size:** 4.
- 971 • **LoRA Configuration:**

972
 973 **Table 11: Performance benchmark on AI-edit video subsets, including five editing types as a**
 974 **supplement to the Table 4 in the main paper.** ♡refers to model zero-shot results. ♦* refers to
 finetuned models.

Dimension	Background		Style Change		Color Change		Action Edit		Object Operation		Overall	
Methods / Metrics	Acc(%)↑	F1↑	Acc(%)↑	F1↑	Acc(%)↑	F1↑	Acc(%)↑	F1↑	Acc(%)↑	F1↑	Acc(%)↑	F1↑
♡MM-Det	95.10	0.935	100.00	1.000	97.67	0.947	96.94	0.960	98.82	1.000	97.85	0.837
♦AIGVDet*	100.0	1.000	100.0	1.000	100.0	1.000	100.0	1.000	100.0	1.000	100.0	1.000
♦MC3_18*	87.37	0.933	95.45	0.977	96.36	0.981	92.78	0.963	92.67	0.962	93.35	0.966

979
 980 **Table 12: Results of cross-generator validation on different training and testing subsets using**
 981 **ResNet3D_18.**

Testing Subset	Training Subset															Avg Acc			
	Alle	Anim	CogV	Hot	LTX	LVDM	LWM	Latt	Lavi	MS	NOVA	T2VZ	Pyra	TAV	VC1	VC2	Wan	ZS	
Allegro	99.3	83.7	3.0	17.0	23.0	0.0	13.0	46.7	44.3	0.3	33.3	79.0	1.0	5.7	0.0	34.0	81.7	3.0	31.6
Animate	49.3	94.7	13.3	26.3	30.0	0.0	34.7	56.3	47.0	1.7	32.0	60.7	0.3	4.7	2.0	19.0	61.0	4.3	29.9
CogVideo	49.7	63.3	99.3	40.0	47.7	0.0	25.7	59.7	66.0	0.3	48.0	40.3	0.0	1.7	1.0	13.7	42.7	3.3	33.5
Hotshot-XL	21.7	47.0	3.7	98.3	46.7	5.7	54.0	73.7	72.0	25.0	67.0	18.0	3.7	4.7	24.7	46.7	18.0	46.0	37.6
LTX	24.0	43.7	4.3	25.7	98.7	0.3	38.0	60.0	34.7	7.3	20.0	27.3	0.7	14.0	2.3	12.3	30.0	4.3	24.9
LVDM	24.0	5.7	0.0	14.3	1.3	100	92.0	83.7	65.0	98.7	11.3	25.7	30.7	24.7	88.3	61.0	31.7	1.3	42.2
LWM	5.7	14.0	0.7	23.3	12.3	18.3	99.7	64.0	15.3	28.0	13.3	14.0	9.7	23.7	10.3	17.7	13.0	1.7	21.4
Latte	41.3	61.3	8.7	27.3	36.7	1.0	59.3	98.7	64.7	9.3	37.0	45.3	5.3	17.3	2.3	41.7	61.7	6.0	34.7
Lavie	55.0	70.0	6.0	32.7	28.7	5.3	44.3	80.0	99.0	4.7	31.0	59.7	3.3	6.0	2.3	49.0	72.3	2.7	36.2
ModelScope	10.0	7.0	0.0	40.0	8.0	81.7	92.7	81.7	28.0	100	28.3	6.3	7.3	12.0	91.7	42.3	12.0	41.3	38.4
NOVA	51.3	68.3	5.7	71.0	54.0	2.3	70.3	71.7	55.3	4.7	99.0	61.0	0.3	3.3	8.7	42.3	34.3	12.7	39.8
Pyramid	96.0	93.0	11.7	27.7	47.3	0.7	19.7	73.3	89.3	0.7	66.0	99.3	3.0	15.0	3.3	72.0	88.0	5.7	45.1
T2V-Zero	30.3	13.0	0.0	3.7	1.7	26.3	76.0	84.3	77.7	26.0	1.0	64.3	98.7	77.0	4.3	52.3	38.7	0.7	37.6
Tune-A-Video	5.7	7.0	0.0	3.0	2.0	4.3	56.7	64.3	20.3	25.3	0.7	32.0	18.0	98.0	7.7	13.3	29.0	6.3	21.9
VideoCrafer1	20.7	30.0	0.0	55.0	23.0	66.0	65.3	62.7	56.7	97.7	53.0	9.7	1.7	9.0	99.3	68.0	25.3	61.0	44.7
VideoCrafer2	59.0	80.0	1.0	75.7	39.3	23.0	72.0	93.7	96.0	26.3	66.3	69.7	9.7	25.7	50.0	99.3	77.3	31.0	55.3
Wan2.1	66.0	82.0	11.3	14.0	24.3	0.3	17.3	67.7	78.3	1.3	19.3	64.0	0.7	8.3	0.3	40.3	98.3	4.3	33.2
ZeroScope	39.3	48.7	1.3	48.7	33.7	0.3	25.0	36.0	44.7	34.0	36.7	24.7	8.7	23.3	52.7	43.7	23	99.3	34.7
ChatGLM	50.7	59.0	4.3	16.0	24.0	1.0	13.7	51.0	65.7	0.3	33.3	53.0	0.0	0.7	3.0	20.0	59.0	2.3	25.4
Gen3	58.0	60.0	0.8	12.2	9.6	0.4	19.5	52.6	50.0	1.0	12.9	67.9	4.0	12.9	1.6	31.5	64.5	1.8	25.6
Genmo	75.7	82.7	1.3	39.0	31.0	1.0	20.7	70.3	75.3	2.0	55.7	81.3	4	8.3	9.0	67.0	75.3	23.7	40.2
Hunyuan	46.7	55.3	1.7	11.3	13.7	0.0	11.3	37.3	44.0	1.0	11.0	50.0	1.0	3.3	0.0	35.3	67.3	2.7	21.8
Hai tuo	48.3	47.3	2.3	9.0	7.7	0.3	17.0	27.7	41.7	0.3	7.0	55.7	3.3	7.7	1.0	28.3	64.0	0.7	20.5
Jimeng	51.3	34.3	0.0	10.7	4.3	0.0	3.0	15.3	19.0	0.0	4.0	46.7	1.0	4.0	1.7	16.3	41.7	2.3	14.2
Kling	38.3	45.0	2.3	23.3	19.0	0.7	15.0	33.3	40.7	2.0	18.0	49.0	1.0	5.3	2.7	31.0	52.0	24.7	22.4
Pixverse	65.7	57.3	1.0	23.3	20.7	0.7	14.0	29.0	50.3	2.3	20.0	75.3	1.0	7.7	3.3	52.3	56.0	9.3	27.2
Sora	47.3	40.0	1.3	14.3	11.7	0.7	12.3	29.0	35.3	1.3	10.7	43.7	1.7	9.0	2.7	20.7	67.7	6.0	19.7
Vidu1.5	60.7	54.7	2.0	4.7	10.3	2.0	14.3	38.0	45.3	1.3	11.3	63.7	1.7	11.3	4.0	44.0	57.7	1.7	23.8
Wanxiang	60.7	72.7	4.0	19.7	19.7	0.3	25.3	53.0	54.0	1.0	26.3	65.3	1.0	7.7	0.7	43.7	81.3	1.7	29.9
Xunfei	58.7	41.3	1.7	22.0	15.0	0.0	6.0	23.3	23.3	0.0	26.3	61.0	0.0	2.3	1.3	31.3	28.7	5.0	19.3
Avg Acc	47.0	52.1	6.4	28.3	24.8	11.4	37.6	57.3	53.3	16.8	30.0	50.5	7.4	15.1	16.1	39.7	51.8	13.9	31.1

- LoRA Rank (lora_rank): 16
- LoRA Alpha (lora_alpha): 16
- Optimizer Settings:
 - Weight Decay (weight_decay): 0.01
 - Warmup Ratio (warmup_ratio): 0.03.

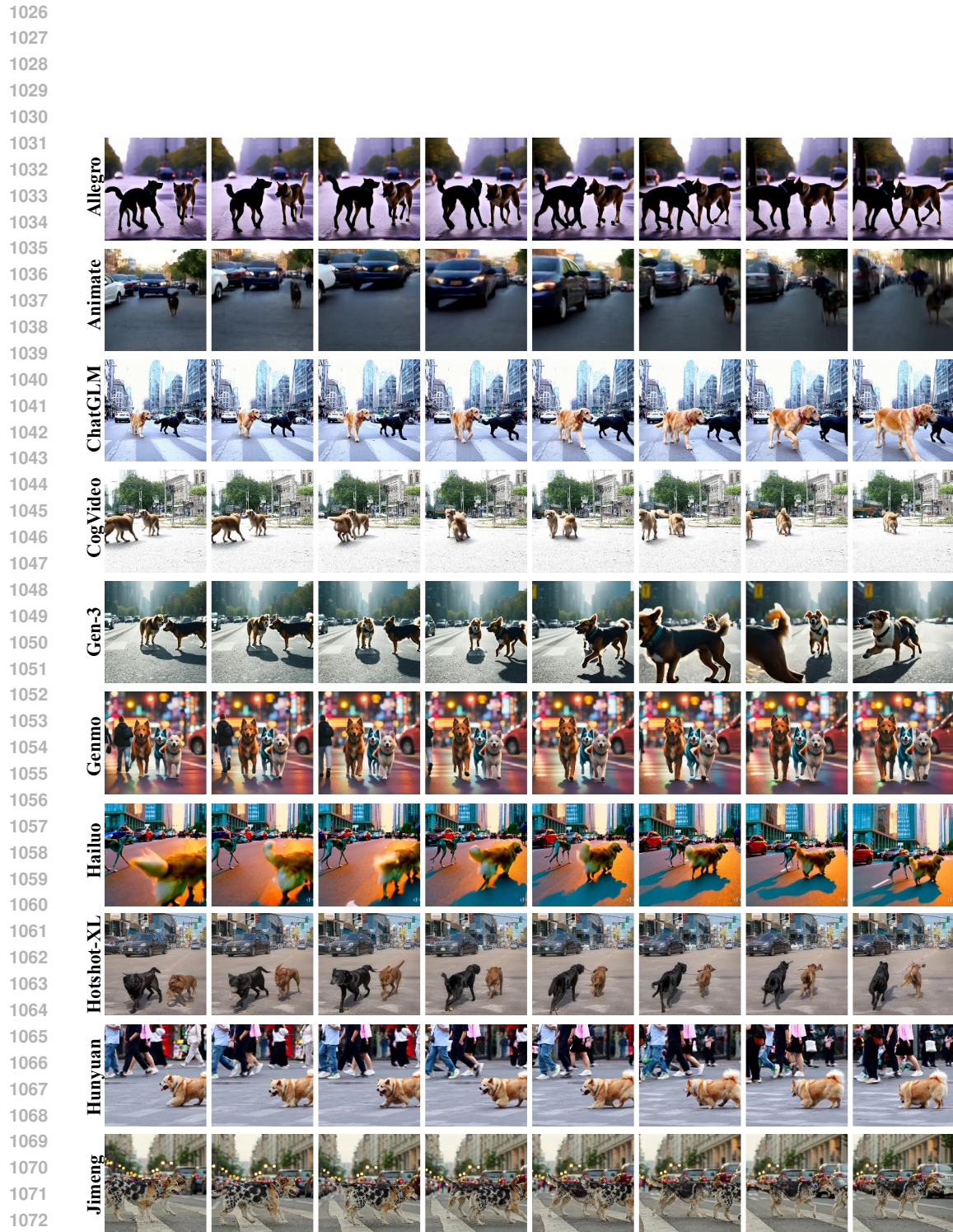


Figure 5: Visualization of the fake video frames in the FVBench dataset generated by different text-to-video generation models with the prompt “two dogs walk across a busy street”.

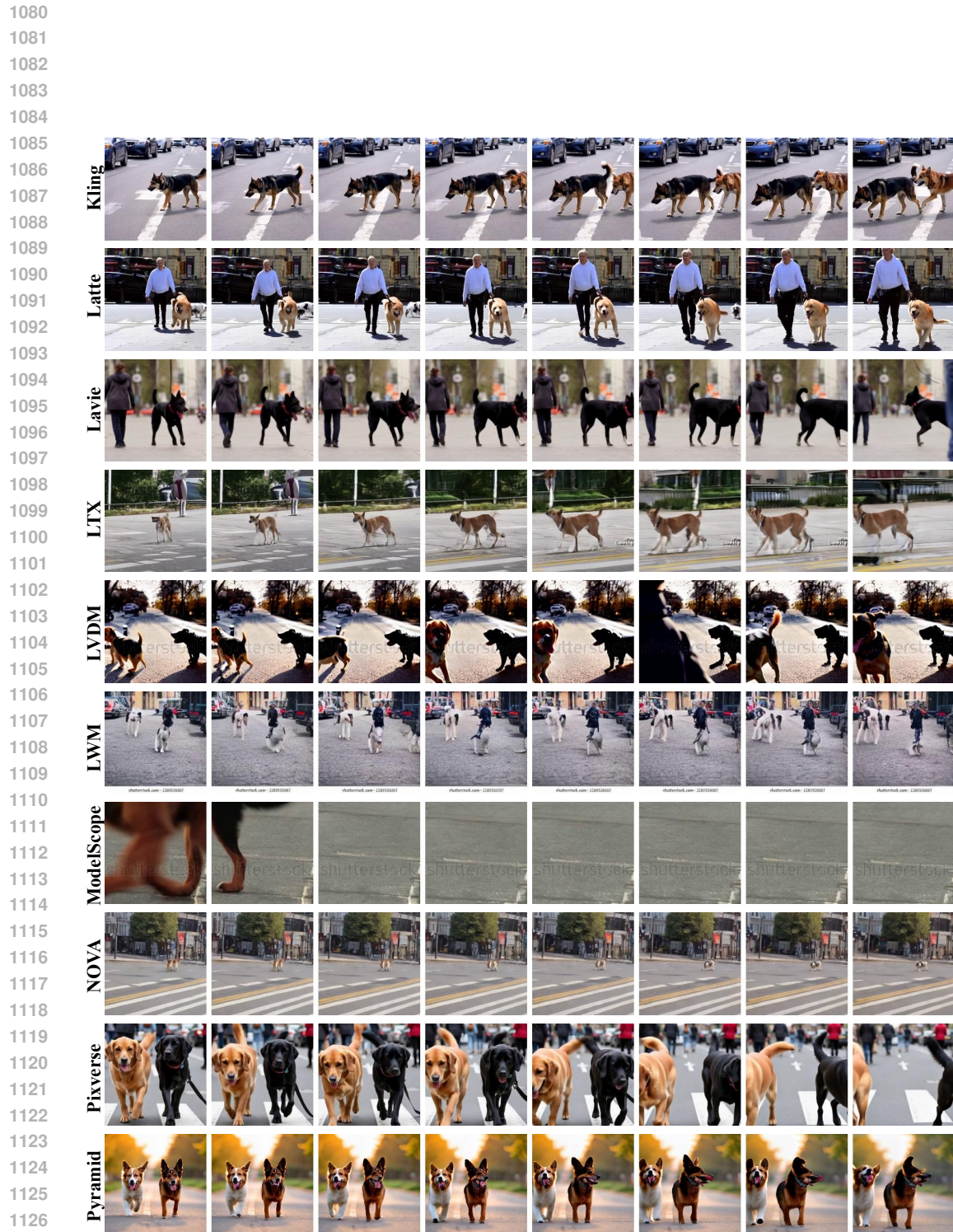


Figure 6: Visualization of the fake video frames in the FVBench dataset generated by different text-to-video generation models with the prompt “two dogs walk across a busy street”.



Figure 7: Visualization of the fake video frames in the FVBench dataset generated by different text-to-video generation models with the prompt “two dogs walk across a busy street”.